Techno-economic assessment of a hydrogen-enriched boiler of 44 MW-thermal power

Master thesis presented by

Eduard Estopañán Moreno

to obtain the master's degree in chemical engineering from the Universitat Rovira i Virgili

Company Supervisor: Francesc Xavier Mas Sotoca

URV Tutor: Joan Manel Vallès Rasquera

Tarragona, January 2023

Acknowledgements

The author sincerely acknowledges the supervision, support and tutelage provided by Mr. Francesc Xavier Mas Sotoca, Mr. Jordi Soler and Dr. Joan Manel Vallès Rasquera.

A very special gratitude goes out to Dr. Martin Demuth, Mr. Marcos Torcal García, Mr. Gustavo Armengou Quintana, Ms. Sílvia Argilaga Monclús and Mr. Carlos Ramos for their help throughout the realization of this work.

The author gratitude extends to Mr. Jaume Aguade and Messer Ibérica de Gases for the funding opportunity to undertake a master's degree at the *Universitat Rovira i Virgili* in Tarragona.

This page intentionally left blank

Index

Nomenclature

Variables

α	Absorptivity	-
ε	Emissivity	-
η	Combustion efficiency	%
$\theta_{N_2,oxi}$	Volume fraction of nitrogen in oxidizer	-
$\theta_{O_2,oxi}$	Volume fraction of oxygen in oxidizer	-
λ	Oxidizer-fuel equivalence ratio	-
λ_w	Thermal conductivity	W/(m·K)
μ_f	Dynamic viscosity of the fluid	Pa·s
ϕ	Ratio of the actual fuel/air ratio to the stoichiometric fuel/air ratio	-
A_s	Total surface area of thermal load	m^2
A_w	Total surface area of firebox walls	m^2
$a_{\alpha,i}$	Absorptivity weighting factor for the i-th grey gas	-
$a_{\varepsilon,i}$	Emissivity weighting factor for the i-th grey gas	-
$b_{\varepsilon,i,j}$	Emissivity gas temperature polynomial coefficient	-
blOPEX	Base line Operating expenses	€/MJ
C	Experimental parameter	-
$\bar{C}_{p,i}\|_{T_{ref}}^{T}$	Specific heat capacity of compound *i*	kJ/(kg·K)
CHF	Critical heat flux	W/m^2
$c_{\alpha,i,j,k}$	Absorptivity polynomial coefficient	-
D_h	Hydraulic equivalent diameter	m
G	Mass flux	$kg/(m^2 \cdot s)$
GWP	Global warming potential	CO_2-e
H	Enthalpy of the output water stream	J/kg
h	Enthalpy of the input water stream	J/kg
h_{fg}	Heat vaporization of water	J/kg

h_{gw}	Convective heat transfer coefficient	W/(m^2·K)
k_i	Absorption coefficient	-
LC	Levelized cost	€/MJ
LFL	Lower flammability limit	%
LHV	Lower heating value	MJ/kg
l_w	Wall thickness	m
MW_i	Molecular weight of compound *i*	kg/kmol
$\dot{m}_i$	Mass flow of compound *i*	kg/s
$\dot{m}_{steam}$	Mass flow of steam at 200ºC	kg/s
P	Partial pressure	Pa
P_{CH_4}	Price of methane (natural gas)	€/Nm^3
P_{CO_2}	Tax price on carbon dioxide emissions	€/kg
P_{H_2}	Price of green hydrogen	€/Nm^3
$\dot{Q}_i$	Heat flow of compound *i*	W
$\dot{Q}_F$	Heat flow of fuel	W
$\dot{Q}_{FG}$	Heat flow of flue gas	W
$\dot{Q}_{Load}$	Heat flow to thermal load	W
$\dot{Q}_{LHV}$	Chemical energy of the fuel based on the lower heating value	W
$\dot{Q}_{OX}$	Heat flow of oxidizer	W
$\dot{Q}_w$	Conductive heat flow through wall	W
$\dot{q}_{abs_g}$	Absorbed heat flux by the flue gas	W/m^2
$\dot{q}_{boiling}$	Boiling heat flux	W/m^2
$\dot{q}_{conv_{gs}}$	Convective heat flux between gas and thermal load	W/m^2
$\dot{q}_{conv_{gw}}$	Convective heat flux between gas and wall	W/m^2
$\dot{q}_{rad_{gs}}$	Radiative heat flux between gas and thermal load	W/m^2

$\dot{q}_{rad_{gw}}$	Radiative heat flux between gas and wall	W/m^2
$\dot{q}_{rad_{ws}}$	Radiative heat flux between wall and thermal load	W/m^2
Re	Reynolds number	-
S	Path length or beam mean length	m
ΔT_{excess}	Excess temperature	K
T_g	Temperature of the exhaust gas (flue gas)	K
T_i	Temperature of compound *i*	K
T_{out}	Outside wall temperature	K
T_{ref}	Reference temperature	K
T_s	Temperature of thermal load	K
T_w	Inside wall temperature	K
UFL	Upper flammability limit	%
X_{H_2}	Hydrogen fraction	%
x_{eq}	Steam quality	-

Acronyms and abbreviations

Ar	Argon
ASU	Air separation unit
CFD	Computational fluid dynamics
CH_4	Methane
CO	Carbon monoxide
CO_2	Carbon dioxide
e^-	Electron
EDR	Exchanger design and rating
GHG	Greenhouse gases
GRG	Generalized Reduced Gradient
H^+	Proton

H_2	Hydrogen
H_2O	Water
He	Helium
HEM	Hydrogen-enriched methane
HENG	Hydrogen-enriched natural gas
IEA	International energy agency
IRENA	International renewable energy agency
KOH	Potassium hydroxide
LCA	Life cycle assessment
LCIA	Life cycle impact assessment
N_2	Nitrogen
NaOH	Sodium hydroxide
NZE	Net zero emissions
O_2	Oxygen
O^{2-}	Oxygen anion
OEC	Oxygen-enhanced combustion
OH^-	Hydroxide anion
PEM	Proton exchange membrane
SDS	Sustainable development scenario
SR	Steam reforming
SRM	Steam reforming of methane
SO_2	Sulphur dioxide
SOEC	Solid oxide electrolyser cell
TEA	Techno-economic assessment
WSGGM	Weighted sum of grey gases model

List of figures

List of tables

Summary

Most industrial boilers require substantial amounts of energy, which are commonly generated by combusting such hydrocarbon fuels as natural gas. However, it suffers from high carbon dioxide (CO_2) emissions problem. Hydrogen (H_2) enrichment of fuels, with hydrogen from renewable sources (the so-called green hydrogen), is currently viewed as an investment priority in the reduction of CO_2 emissions.

This work examines the techno-economic feasibility of implementing hydrogen-enriched methane (HEM) for heat production in an industrial O-type water-tube boiler of 44 MW-thermal power.

Results show that the combustion efficiency (or available heat) increases from 52.43% (with 0 vol% hydrogen) to 55.97% (with 80 vol% hydrogen). Also, that the economic feasibility of using HEM as fuel for industrial boilers depend predominantly on carbon taxes and green hydrogen pricing.

From an economic point of view, green hydrogen could represent a promising fuel for 2030 in scenarios where its production cost is low (≤3 €/kg H_2) and taxes on carbon emissions are relatively high (~0.13 €/kg CO_2). However, this research has shown that a sustained decline in natural gas prices, diminishes significantly the incentives for using green hydrogen as fuel in 2030.

Nonetheless, whether the Net Zero Emissions by 2050 scenario is achieved, then HEM for heat production in industrial boilers is largely economically viable, because green hydrogen production costs are low and carbon taxes are sufficiently high. Risk analysis show that only in 18% of the future projection cases for 2030, using a mixture of 40-60 hydrogen-methane will be more expensive than pure methane.

From an environmental perspective, to produce 1 kg of steam at 200ºC from solely natural gas (methane), 437.8 g CO_2-e are emitted to the atmosphere; whereas, to produce 1 kg of steam from a mixture of 80-20 hydrogen-methane, 206.1 g CO_2-e are produced. This represents a decrease of 53% of carbon emissions.

These findings are essential for industry and policymakers to enable lower greenhouse gas (GHG) emissions and achieve climate neutrality.

1. Introduction

1.1. Context of the study

Earth's climate system has evolved over many millions of years, and evidence from natural archives provides a long-term perspective on observed changes and projected changes over the coming centuries (Intergovernmental Panel on Climate Change (IPCC), 2021). These data also show that atmospheric carbon dioxide concentrations and global surface temperature are strongly coupled.

Carbon dioxide (CO_2) is an important heat-trapping gas, which is released through human activities such as deforestation and burning fossil fuels, as well as natural processes such as respiration and volcanic eruptions. Figure 1 shows atmospheric CO_2 levels measured at Mauna Loa Observatory, Hawaii, in recent years. The concentration of CO_2 in the atmosphere has increased from a pre-industrial value of 280 ppm to more than 400 ppm in 2020 (Huisingh et al., 2015).

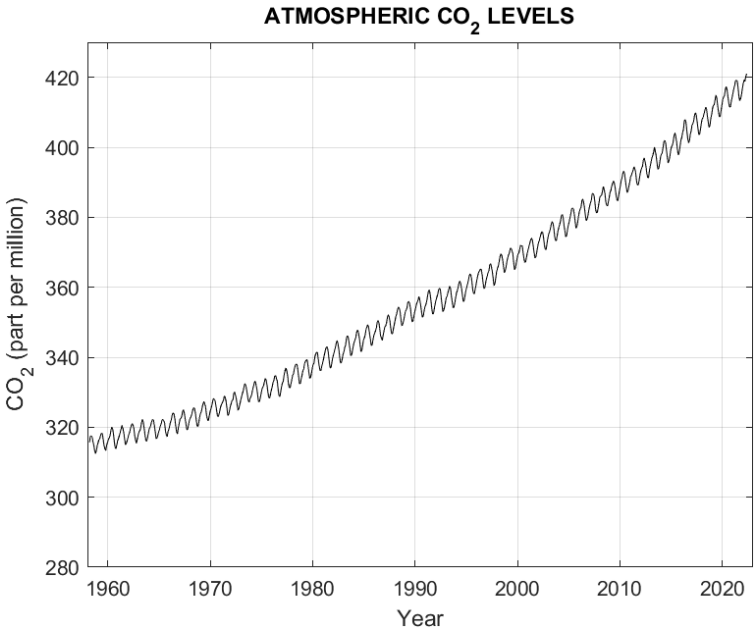

Figure 1. Atmospheric CO_2 levels measured at Mauna Loa Observatory, Hawaii. Data source: http://www.noaa.gov/

Since the beginning of the industrial era (1760), human activities have raised atmospheric concentration of CO_2 by about 50%. Furthermore, the evidence for human influence on the climate system was found to have progressively strengthened (Eyring et al., 2021). Earth's surface continues to significantly warm, with recent global temperatures being the hottest in the past 2000-plus years.

Figure 2 illustrates the change in global surface temperature relative to 1951-1980 average temperatures. Nineteen of the hottest years have occurred since 2000.

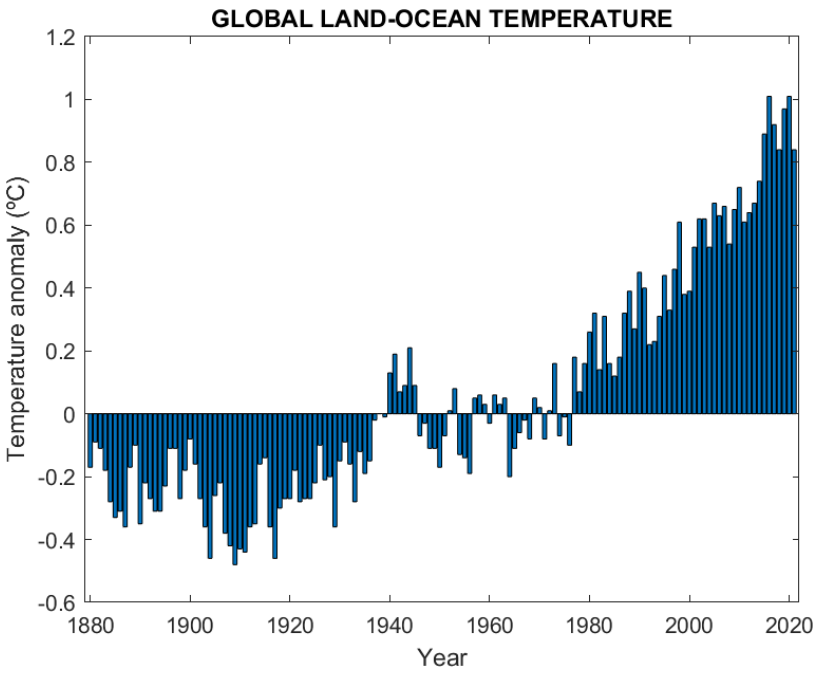

Figure 2. Change in global surface temperature. Data source: NASA's Goddard Institute for Space Studies (GISS).

The environmental consequences of global warming, such as sea-level rise, flooding, drought, heat waves, intense storms and degraded air quality are a great challenge to the present generation (Eyring et al., 2021). Thus, the reduction of greenhouse gases is of vital importance to limit the long-term global temperature increase (Intergovernmental Panel on Climate Change (IPCC) Special Report, 2008).

Hydrogen (H_2) is one of the most promising clean and sustainable energy carriers. H_2 has a high energy density (140 MJ/kg) which is more than two times higher than typical fossil fuels (50 MJ/kg) (Chi & Yu, 2018). Furthermore, H_2 combustion does not produce carbon emissions.

The decarbonization of energy systems is considered to be a critical problem by the European Commission. Consequently, on July 8, 2020, the EU Hydrogen Strategy was presented, highlighting hydrogen as an investment priority in the framework of the European Green Deal (European Commission, 2020).

Currently the produced hydrogen is mostly used in industrial applications, such as fertilizers, petroleum refining processes, petrochemical, fuel cells, and chemical industries.

Hydrogen is produced from various renewable and non-renewable energy resources such as fossil fuels, especially steam reforming of methane (SRM). Unfortunately, more than 90% of the global hydrogen production comes from SRM according to the cited literature (Lee et al., 2018).

Figure 3 shows the various comprehensive hydrogen production methods.

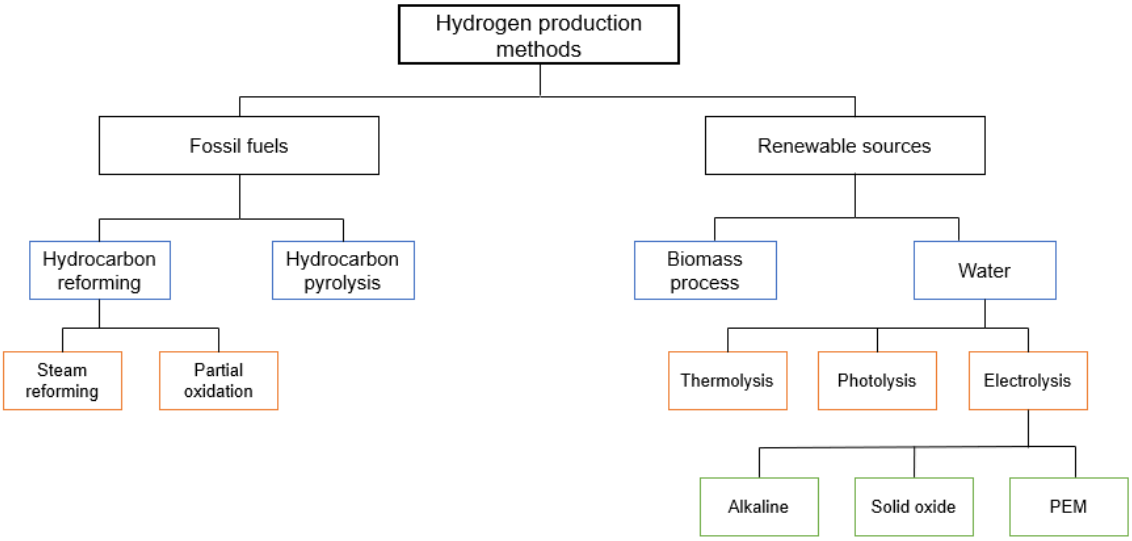

Figure 3. Hydrogen production methods. Data from cited literature (Shiva Kumar & Himabindu, 2019a).

1.2. Hydrogen production technologies

H_2 can be produced from many different renewable and non-renewable feedstocks and technological pathways, with widely varying GHG emissions. For hydrogen to have a role in future low-carbon energy systems, it is necessary to demonstrate that it has sufficiently low carbon emissions.

Nonetheless, producing hydrogen from non-renewable sources is the most developed and commonly used approach and basically include hydrocarbon reforming and hydrocarbon pyrolysis (Newborough & Cooley, 2020).

Although hydrocarbons are currently the main feedstock used for H_2 production, the need to increase renewable technologies will become unavoidable. The share of renewable technologies will increase in the near future while in long term, is expected to dominate over conventional technologies (Muradov & Veziroğlu, 2005).

1.2.1. Hydrocarbon reforming

Hydrocarbon reforming is the process by which the hydrocarbon fuel is converted into hydrogen through some catalytic techniques. In addition to the hydrocarbon, the other reactant for the reforming process can be either steam, and then the endothermic reaction is known as steam reforming, or oxygen, and the exothermic reaction is known as partial oxidation.

Steam reforming (SR) is the most used method and basically involves a catalytic conversion of the hydrocarbon and steam to hydrogen and carbon oxides. In order to produce the desired purified H_2 product and prevent coking formation on the catalyst surface, the operation parameters of reforming reaction are selected at high temperatures, pressures up to 3.5 MPa and steam-to-carbon ratios of 3.5 (Ersöz, 2008).

Figure 4 shows a flow diagram of the SRM process.

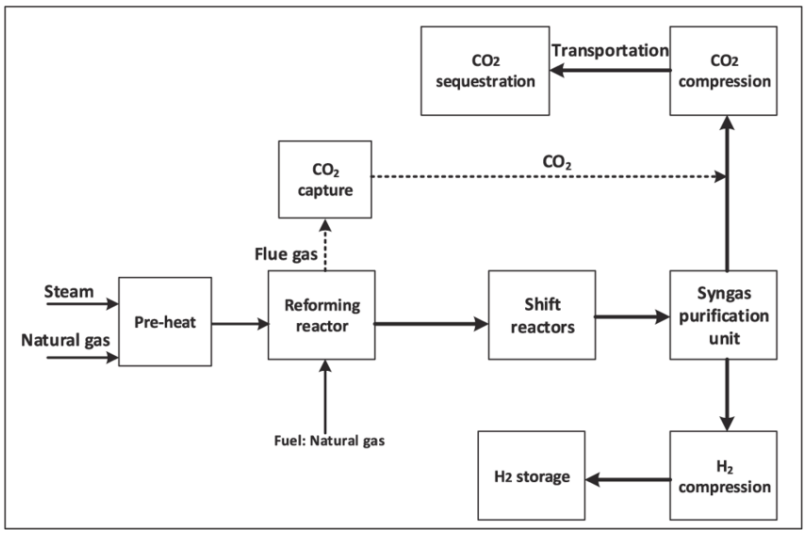

Figure 4. Flow diagram of the SRM process (Oni et al., 2022).

The main chemical reactions that take place in SR are shown in Equation 1, Equation 2 and Equation 3 (Bion et al., 2010).

$$C_nH_m + nH_2O \rightarrow nCO + \left(n + \frac{1}{2}m\right)H_2 \quad \text{Equation 1}$$

$$C_nH_m + 2nH_2O \rightarrow nCO_2 + \left(2n + \frac{1}{2}m\right)H_2 \quad \text{Equation 2}$$

$$CO + H_2O \rightarrow CO_2 + H_2 \quad \text{Equation 3}$$

1.2.2. Hydrocarbon pyrolysis

Hydrocarbon pyrolysis is a well-known process in which the only source of hydrogen is the hydrocarbon itself, which undergoes thermal decomposition through the general reaction shown in Equation 4.

$$C_nH_m \rightarrow nC + \frac{1}{2}mH_2 \quad \text{Equation 4}$$

From environmental points of view, it would be more advantageous to produce both hydrogen and carbon by the catalytic dissociation of natural gas, as opposed to the production of hydrogen by SRM coupled with CO_2 sequestration (Muradov & Veziroğlu, 2005). And if a market for the huge amounts of carbon that will be produced by decomposition of natural gas was found, the price of hydrogen would be further reduced.

1.2.3. Hydrogen from renewable sources

Hydrogen obtained from renewable energy sources is classified as green H_2 (Velazquez Abad & Dodds, 2020), whereas hydrogen obtained from hydrocarbons is classified as grey H_2. However, if hydrogen is obtained from hydrocarbons but carbon capture, utilization and storage technologies are employed, then the hydrogen is classified as blue H_2. Figure 5 shows a scheme of the types of hydrogen.

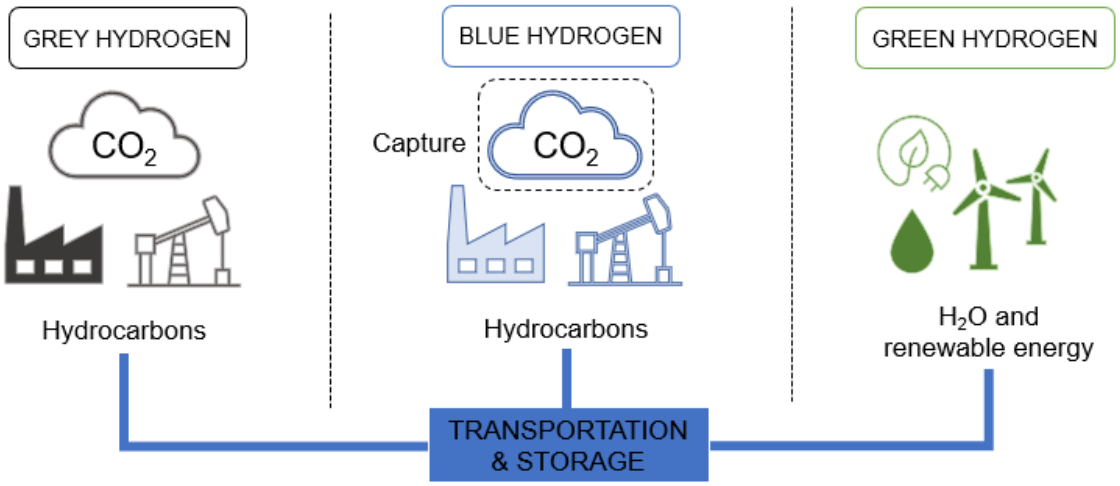

Figure 5. Types of hydrogen according to raw material.

Hydrogen production from renewable sources is mainly limited to biomass processes and water splitting processes, which include thermolysis, photolysis and electrolysis (Nikolaidis & Poullikkas, 2017).

Water electrolysis technologies have gained special attention in the last few years, mainly thanks to the possibility of approaching commercial markets.

1.2.3.1. Water electrolysis

Water is one of the most abundant and inexhaustible raw materials on Earth and can be used for H_2 production through water-splitting processes such as electrolysis, thermolysis and photolysis. If the required energy input is provided from renewable energy sources, the hydrogen produced will be the cleanest energy carrier that could be used by humankind.

Electrolysis is an established and well-known method, constituting the most effective technique for water splitting. The reaction, however, is very endothermic and the simplest way of providing the energy needed is by running the reaction electrochemically (Rossmeisl et al., 2005).

A typical electrolysis unit or electrolyser consists of a cathode and an anode immersed in an electrolyte, and generally when electrical current is applied, water splits and hydrogen is produced at the cathode while oxygen is evolved on the anode.

Currently, the developed and commonly used electrolysis technologies are alkaline, proton exchange membrane (PEM) and solid oxide electrolysis cells (SOEC).

- Alkaline electrolysis operates at low temperatures (30 – 80 ºC) with aqueous solution (KOH/NaOH) as the electrolyte (de Groot et al., 2022). The reactions that take place in the cell are:

$$\text{Anode: } 2OH^- \rightarrow H_2O + \frac{1}{2}O_2 + 2e^- \qquad \text{Equation 5}$$

$$\text{Cathode: } 2H_2O + 2e^- \rightarrow H_2 + 2OH^- \qquad \text{Equation 6}$$

- PEM electrolysis operates at low temperatures (20 – 80 ºC) and high pressure (Shiva Kumar & Himabindu, 2019b). The following reactions are carried out:

$$\text{Anode: } H_2O \rightarrow 2H^+ + \frac{1}{2}O_2 + 2e^- \quad \text{Equation 7}$$

$$\text{Cathode: } 2H^+ + 2e^- \rightarrow H_2 \quad \text{Equation 8}$$

- Solid oxide electrolysis operates at high pressure and high temperatures (500 – 850 ºC) and utilizes water in form of steam (Götz et al., 2016). Here the reactions are:

$$\text{Anode: } O^{2-} \rightarrow \frac{1}{2}O_2 + 2e^- \quad \text{Equation 9}$$

$$\text{Cathode: } H_2O + 2e^- \rightarrow H_2 + O^{2-} \quad \text{Equation 10}$$

1.3. Combustion in burners

Most industrial burners require substantial amounts of energy, which are commonly generated by combusting such hydrocarbon fuels as natural gas or oil. Most combustion processes use air as the oxidant. Air consists of approximately 78% nitrogen, 21% oxygen and 1% argon. In many cases, these processes can be enhanced by using an oxidant that contains a higher proportion of oxygen (O_2), this is known as oxygen-enhanced combustion (OEC).

Another example uses high-purity oxygen as the oxidant, instead of air. This is usually referred to as oxy-fuel combustion (Smith et al., 2018).

New oxygen generation technologies, such as pressure and vacuum swing adsorption have significantly reduced the cost of separating oxygen from air (Chang et al., 2021). Another important development is that OEC can reduce pollutant emissions.

Nitrogen in air acts as a ballast that carries energy out with the exhaust (Baukal, 1998). The available heat increases significantly when pure oxygen is used as oxidant. The available heat (%) is calculated as the ratio of the amount of heat released by a specified quantity of fuel (heating capacity) less the energy carried out by the exhaust gas, and the lower heating value of this specified quantity, as shown in Equation 11.

$$\text{Available heat (\%)} = \frac{\dot{Q}_{LHV} + \dot{Q}_F + \dot{Q}_{OX} - \dot{Q}_{FG}}{\dot{Q}_{LHV}} \cdot 100 \quad \text{Equation 11}$$

Where $\dot{Q}_{LHV}$ is the chemical energy (represented by the lower heating value or LHV) of the inlet fuel, $\dot{Q}_F$ is the heat flow of the inlet fuel, $\dot{Q}_{OX}$ is the heat flow of the oxidizer (e.g., air or oxygen) and $\dot{Q}_{FG}$ is the heat flow of the exiting flue gas.

Figure 6 shows the available heat for the combustion of methane as a function of the oxygen concentration in the oxidizer for three different exhaust gas temperatures. As the exhaust gas temperature increases, the available heat decreases because more energy is carried out the exhaust stack.

And Figure 7 shows how the available heat, for stoichiometric air/methane and oxygen/methane flames, varies as a function of the exhaust gas temperature. As the exhaust temperature increases, more energy is carried out of the combustion system and less remains in the system.

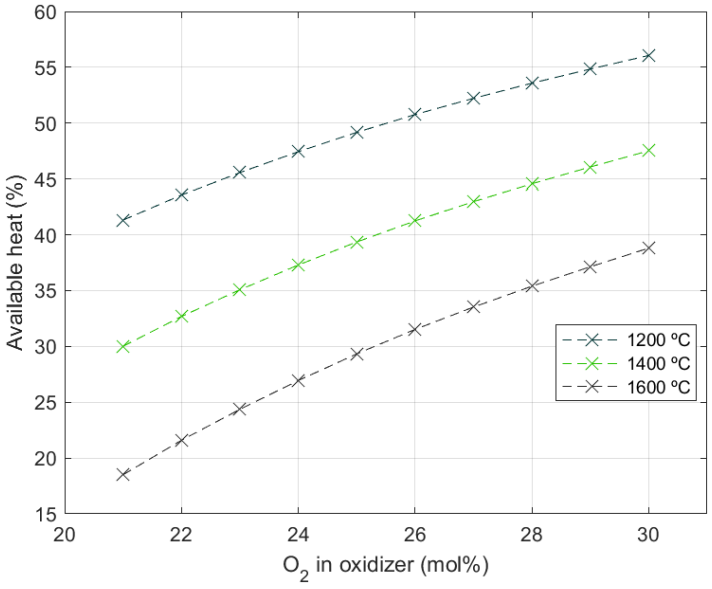

Figure 6. Available heat vs. oxidizer composition, for a stoichiometric CH_4 flame, at exhaust temperatures of 1200, 1400 and 1600ºC without flue gas recuperation.

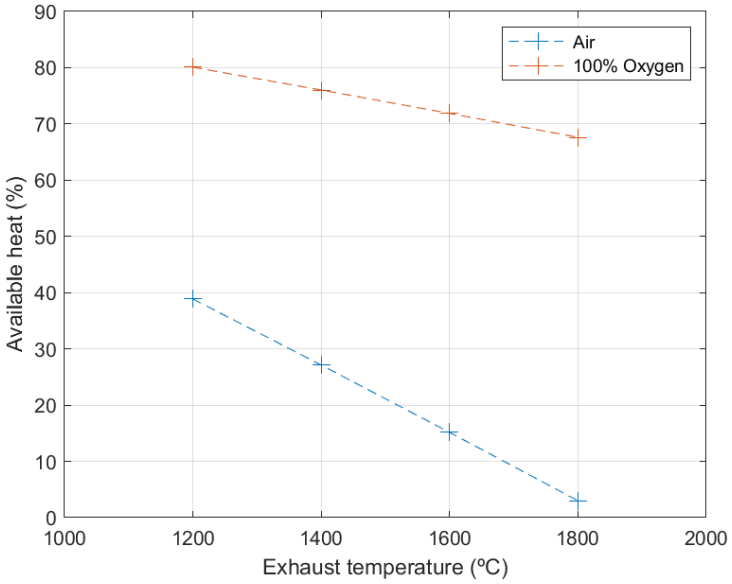

Figure 7. Available heat vs. exhaust gas temperature, for a stoichiometric CH_4 flame with air and pure oxygen as oxidant, without flue gas recuperation.

The upper flammability limit increases linearly with the O_2 concentration in the oxidizer, while the lower flammability limit is nearly constant for oxidizers with more than about 35% O_2 in the oxidizer according to the cited literature (Baukal, 1998). Table 1 shows examples of the way using O_2 instead of air widens the flammability range for a given fuel.

Table 1. Flammability and detonability limits of hydrogen and methane in air and oxygen (Green et al., 2019).

	Flammability limits (mol%)	Detonability limits (mol%)
H_2-Air	4-75	20-65
H_2-O_2	4-95	15-90
CH_4-Air	5-15	6-14
CH_4-O_2	5-61	10-50

OEC is used in a wide range of industrial heating applications. In general, OEC is currently used in high-temperature heating and melting processes that are either very inefficient or not possible with air/fuel combustion.

According to the cited literature, (Raič et al., 2021) and (Raič et al., 2022), oxy-fuel combustion has experienced a wide-spread adoption in the glass industry, largely thanks to the growing sophistication of Computational Fluid Dynamics (CFD) simulations.

1.3.1. Combustion of hydrogen-enriched methane

As mentioned before, hydrogen is an attractive fuel from an environmental perspective as it emits only water as by-product. However, there are several difficulties associated with using pure hydrogen as a fuel including its production, safety, quick charge capability, low-temperature discharge characteristics, and low density, which limits its storage capabilities (Bălănescu & Homutescu, 2021).

Therefore, hydrogen enrichment of fuels is currently assumed to be in a transitional stage (Sørensen, 2012). In addition to carbon emission reduction, the addition of hydrogen to methane changes the combustion characteristics such as the adiabatic flame temperature, flame velocity, flame stability, and flame propagation. However, according to (Zhao et al., 2019a), these changes can be insignificant at low hydrogen fractions, below 15% volume fraction. But when the hydrogen fraction is increased beyond this threshold, the stability of the flame increases thanks to the enhancement of both the autoignition process and the flame velocity (Hawkes & Chen, 2004).

The recent literature reporting flammability limit data of hydrogen/methane/air mixtures was summarized in a flammability regime diagram in the parameter space of hydrogen fraction X_{H_2} and equivalence ratio ϕ (ratio of the actual fuel/air ratio to the stoichiometric fuel/air ratio), as shown in Figure 8.

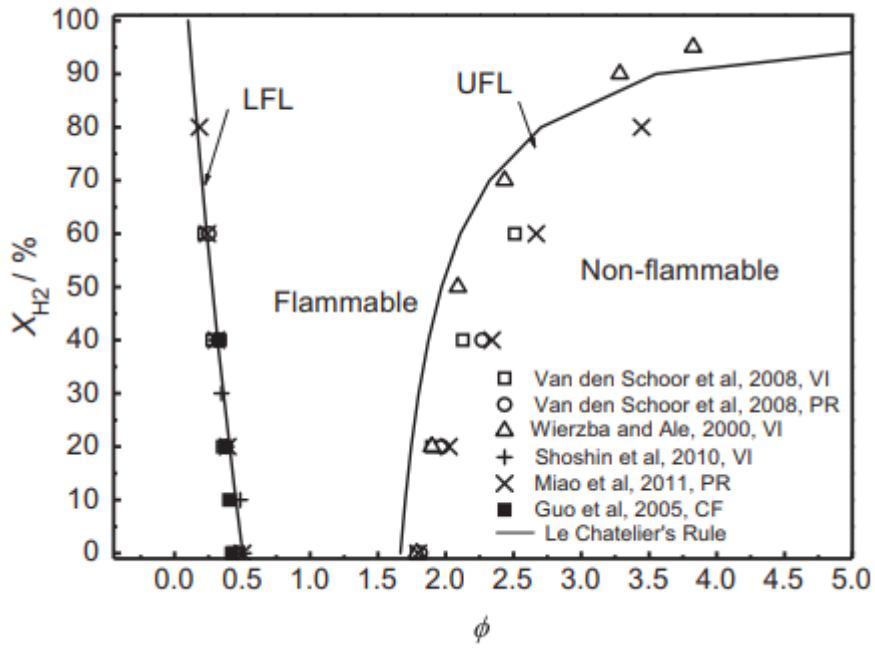

Figure 8. Flammability region diagram for methane/hydrogen/air mixture at 1 atm and 25ºC (Tang et al., 2014).

Experimental results from (Ge et al., 2019) indicate that the flame shrinks distinctly when the addition of hydrogen is increased to certain content. To be specific, the flame structure changes little as the hydrogen content is lower than 5%, and the flame expanding angle also keeps well. Once the hydrogen concentration is boosted to be over 11%, the flame expands greatly towards the confinement wall.

Moreover, according to (Zhao et al., 2019b), the burner temperature is 63% higher when the hydrogen volume fraction in the fuel was 10%, compared to that of pure methane.

Overall, hydrogen enrichment affects the combustion instability of a combustor with partial premixing, as stated in (Y. Zhang et al., 2019), and increases the flow velocity in the combustion chamber and reduces the flame density, thereby, broadening the structure of the diffusion flame.

With addition of hydrogen to hydrocarbon fuels, the fuel composition changes, causing an effect on both the chemical and physical processes. These variations mainly influence the flame stability, pollutant emissions and combustion efficiency (Wierzba & Ale, 2000).

1.4. Heat transfer in combustion chambers

Radiation is a dominant heat transfer mode in combustion chambers as compared with convection and conduction transfers (Ebrahimi et al., 2013). In fact, energy transfer by radiation is the fastest of all energy transfer mechanisms. Also, radiation transfer occurs in solids as well as liquids and gases. Thermal radiation is emitted because of energy transitions of molecules, atoms, and electrons of a substance (Cengel, 2002).

A body at a temperature above absolute zero emits radiation in all directions over a wide range of wavelengths. The amount of radiation energy emitted from a surface at a given wavelength depends on the material of the body and its surface temperature (Lienhard, 2019).

When radiation strikes a surface, part of it is absorbed, part of it is reflected, and the remaining part, if any, is transmitted (Figure 9).

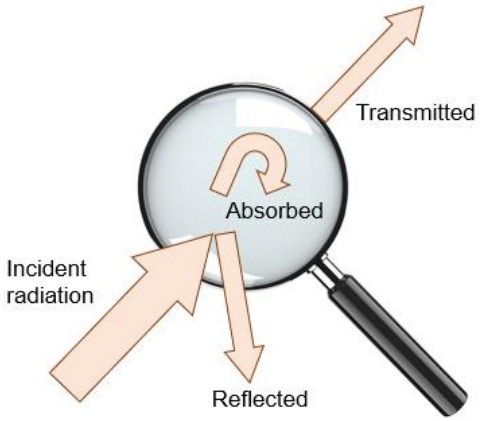

Figure 9. Absorption, reflection and transmission of incident radiation.

Note that surfaces emit radiation as well as reflect it, and thus the radiation leaving a surface consists of emitted and reflected parts. During a radiation interaction, a surface loses energy by emitting radiation and gains energy by absorbing radiation emitted by other surfaces (Green et al., 2020).

1.4.1. Radiation from gases

Gases that consist of monoatomic molecules such as Ar and He and symmetric diatomic molecules such as N_2, O_2 and H_2 are essentially transparent to radiation, except at extremely high temperatures at which ionization occurs.

Nonetheless, gases with asymmetric molecules such as H_2O, CO_2, CO, SO_2, and hydrocarbons may participate in the radiation exchange process by absorption and emission at high temperatures such as those found in combustion chambers. Many scientists attempted to model an analysis of the radiative environments (Modest et al., 2013).

Thus, radiant transfer in a gaseous medium is characterized by the gas emissivity and gas absorptivity. The gas emissivity is a function of only the gas temperature while the absorptivity is function of both the gas temperature and a surface irradiation temperature.

1.4.2. Radiative gas property models

The presence of a participating medium complicates the radiation analysis considerably for several reasons:

- Gases emit and absorb radiation at a number of narrow wavelength bands. This is in contrast to solids, which emit and absorb radiation over the entire spectrum.
- The emission and absorption characteristics of the constituents of a gas mixture depend on the temperature, pressure, and composition of the gas mixture.

Radiative gas property models which yield total emissivities and absorptivities may be classified into four general categories associated with narrow-band models (Ludwig et al., 1973), exponential wide-band models (Edwards, 1976), weighted sum of grey gases models (Cassol et al., 2014; Hottel H.C., 1969), and charts and correlations (de Ris, 1984).

Evaluation of radiant exchange within a gas as well as between a gas and surrounding surfaces may be accomplished by the zone method (Ebrahimi et al., 2013).

The zone method minimizes the computational effort by introduction of the weighted sum of grey gases model for the radiative properties of total emissivity and absorptivity. Grey gas emissivities are expressed in terms of a temperature independent grey gas absorption coefficient and the product of the partial pressure of the absorbing gas and path length.

1.4.2.1. Weighted sum of grey gases model (WSGGM)

Total emissivity for the weighted sum of grey gases model is evaluated from Equation 12.

$$\varepsilon = \sum_{i=1}^{I} a_{\varepsilon,i}(T) \cdot [1 - e^{-k_i PS}] \qquad \text{Equation 12}$$

Where $a_{\varepsilon,i}$ denotes the emissivity weighting factors for the i-th grey gas as based on gas temperature (T). The bracketed quantity denotes the i-th grey emissivity with absorption coefficient, k_i, and partial pressure-path length product, PS (Yuen, 2008). For a gas mixture, P is the sum of the partial pressures of the absorbing gases. And for an arbitrary shape of volume V and surface area A, the path length is calculated as 3.6V/A (Cengel, 2002).

A convenient representation of the temperature dependency of the weighting factors is a polynomial of order J-1 (Green et al., 2020), as shown in Equation 13.

$$a_{\varepsilon,i} = \sum_{j=1}^{J} b_{\varepsilon,i,j} \cdot T^{j-1} \qquad \text{Equation 13}$$

Where $b_{\varepsilon,i,j}$ are referred to as the emissivity gas temperature polynomial coefficients.

For total absorptivity, the irradiation temperature of surfaces surrounding the gas is also introduced, as depicted in Equation 14.

$$\alpha = \sum_{i=1}^{I} a_{\alpha,i}(T, T_s) \cdot [1 - e^{-k_i PS}] \qquad \text{Equation 14}$$

Where the absorptivity weighting factors, $a_{\alpha,i}$, are also a function of the surface irradiation temperature, T_s. The weighting factors must all be positive.

The dependency of the weighting factors on gas and irradiation temperature is expressed by polynomials of orders J-1 and K-1, as shown in Equation 15.

$$a_{\alpha,i} = \sum_{j=1}^{J}\left[\sum_{k=1}^{K} c_{\alpha,i,j,k} {T_s}^{k-1}\right] T^{j-1}$$ Equation 15

Where $c_{\alpha,i,j,k}$ are the absorptivity polynomial coefficients. In order to reduce the computational effort associated with the zone method, the absorption coefficients for total emissivity and absorptivity are taken to be identical (Smith T. F. et al., 1982).

1.5. Boilers: state of the art

A boiler is a closed vessel in which a fluid is heated, generally water. Then the heated or vaporized fluid exits the boiler for use in various processes or heating applications (ASME PTC 4-2008, 2009).

Boilers can be classified into two main groups (Dukelow, 1991):

- Fire-tube boilers: water partially fills the vessel with a small volume left above to accommodate the generated steam. The heat source is inside a furnace that is always surrounded by water (Figure 10a). Fire-tube boilers usually have a comparatively low rate of steam production, but high steam storage capacity.
- Water-tube boilers: tubes filled with water are arranged inside a furnace in a few possible configurations. The water-tubes connect large drums, one containing water located at the bottom and the other containing water and steam located at the top (Figure 10b). This type generally gives high steam production rates, but less storage capacity and are mostly preferred in high-pressure applications (Heselton, 2005). There are mainly two types of water-tube boilers; the so-called O-type boilers that have a cylindrical shape and the D-type boilers that have a D form frontal section.

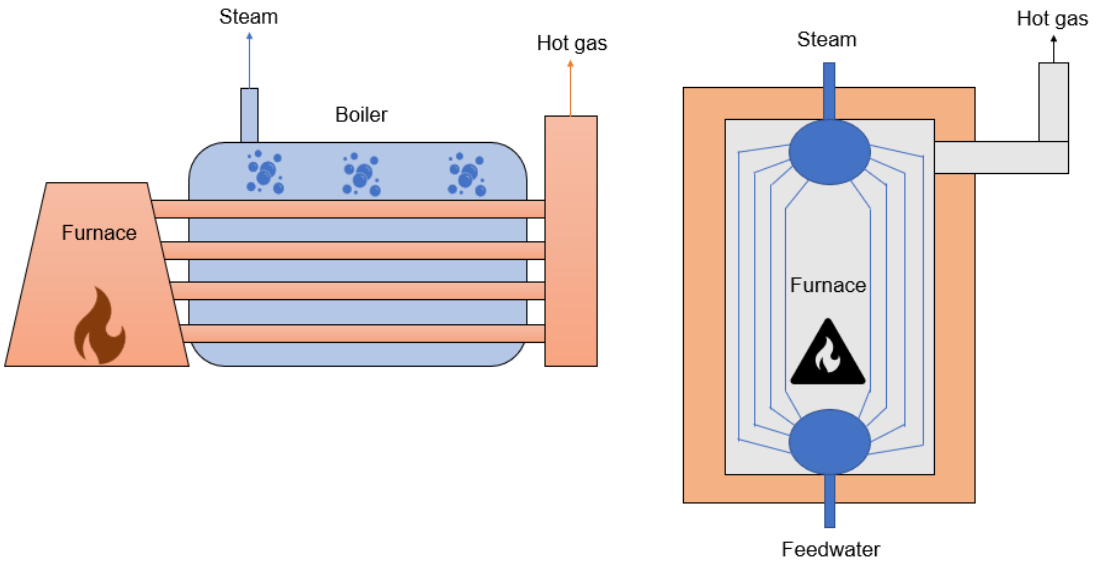

(a) (b)

Figure 10. Schemes of (a) Fire-tube boiler and (b) Water-tube boiler.

The understanding of critical heat flux (CHF) is paramount in gas-fired boilers.

The CHF phenomenon was discovered when Nukiyama did an experimental study on the maximum heat flux value in saturated pool boiling of water in connection with the problem of increasing the evaporation rate of marine boilers (Nukiyama, 1934).

Figure 11 demonstrates that after the excess temperature (ΔT_{excess}) has reached a certain limit, the heat flux transmitted from a metal surface to the boiling water $\dot{q}_{boiling}$ decreases with further increase in ΔT_{excess}. The heat flux at this point is called critical heat flux or CHF.

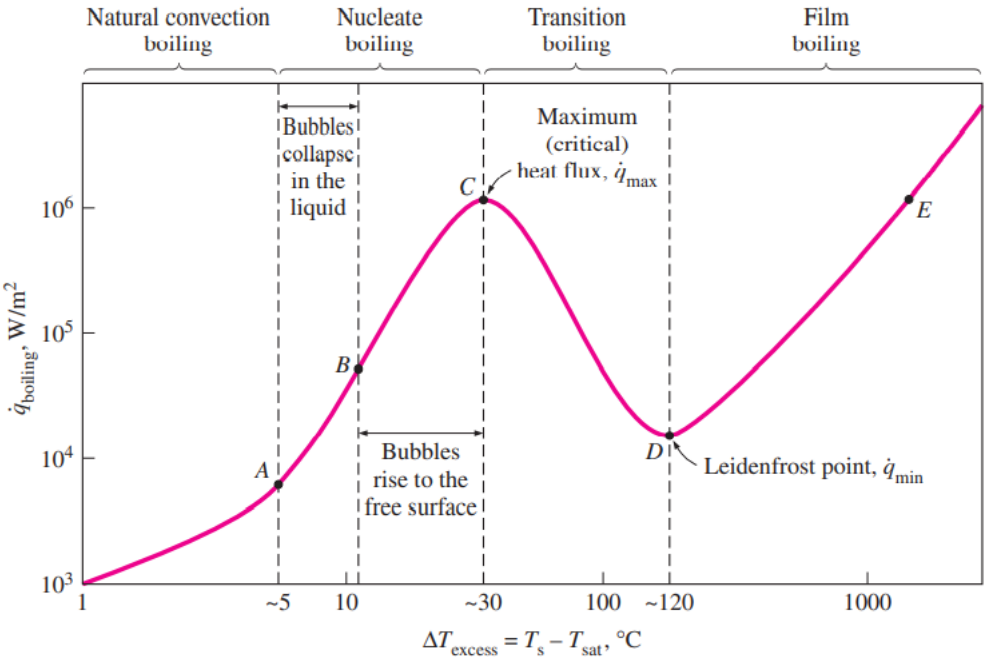

Figure 11. Nukiyama's boiling curve for saturated water at 1 atm (Cengel, 2002).

Water will go through the regimes of natural convection boiling (heat transfer from the heating surface to the fluid is by natural convection, to point A), nucleate boiling (formation of bubbles at different rates, between points A and C), transition boiling (as the heater temperature is increased, the heat flux decreases because of the formation of a vapor film on the heater surface, between points C and D) and film boiling (the heater surface is completely covered by a vapor film, beyond point D).

In view of practical significance of a correlation of CHF in the aspects of engineering design and prediction, several studies investigated this phenomenon and came up with different correlations (Harnett & Irvine, 1985; Novak Zuber June, 1959; W. Zhang et al., 2006).

1.5.1. Hydrogen-enriched methane (HEM) combustion in boilers

Several scientists have focused on the hydrogen-methane mixture implications on end-user devices such as boilers (Io Basso et al., 2017) (Tang et al., 2014).

(Wang et al., 2022) studied the efficiency and emissions of a gas-fired industrial boiler fuelled with hydrogen-enriched natural gas (HENG).

(Bălănescu & Homutescu, 2021) investigated the use of hydrogen-enriched methane as a fuel in condensing boilers. The results demonstrated that the condensing boiler efficiency in terms of the higher heating value increased by 1.3%, owing to the additional latent energy saved as the hydrogen volumetric fraction increased from 0% to 80%.

2. Scope of the project and specific objectives

This study aims to investigate the technical and economic feasibility of an O-type water-tube boiler fuelled with HEM. Tubes filled with water are arranged inside a furnace. The water-tubes connect large drums, one containing water located at the bottom and the other containing water and steam located at the top.

The internal dimensions of the furnace are 6000 mm of inner diameter and 18000 mm long which is insulated by a ceramic insulation of 200 mm. The furnace is equipped with one forced drought standard burner that has a diameter of 500 mm. The water-tube nominal bore is approximately 90 mm, and the total surface area of the tubes is 538.7 m^2.

Hydrogen from renewable sources blended with methane will be used as fuel to produce steam at 200ºC in a water-tube boiler of 44 MW of thermal power. The ultimate objective is to compare the techno-economic aspects of the aforementioned boiler if only methane is used as fuel, and if HEM (at different ratios) is employed.

Figure 12 depicts the characteristics of the boiler.

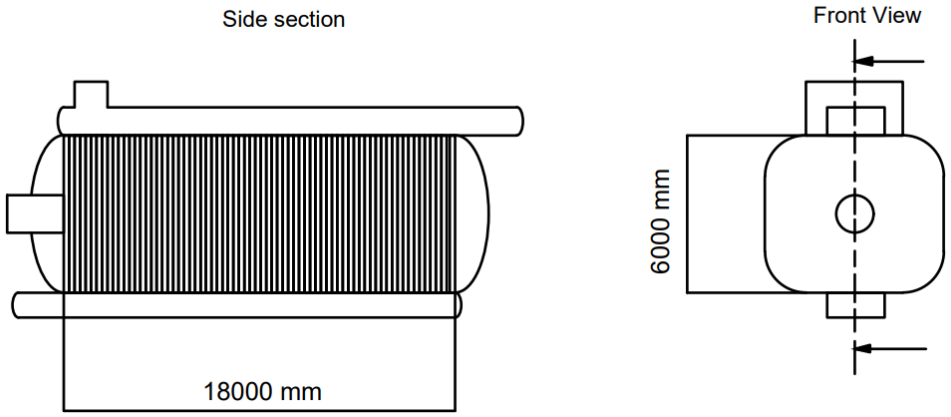

Figure 12. Simplified scheme of the O-type water-tube boiler of study.

The specific objectives of this study are:

- Assess the economic feasibility of using green hydrogen as fuel in a water-tube boiler. Study the evolution of hydrogen, methane (main component of natural gas), electricity and carbon dioxide tax prices in the European Union and, ultimately, Spain.
- Compare the economic aspects of the boiler if only methane is used as fuel, and if HEM (at different ratios) is employed.
- Evaluate the mass and energy balance of a water-tube boiler of 44 MW-t. And assess the technical aspects of a hydrogen-methane mixture, at different ratios, associated with combustion and heat transfer.
- Do a sensitivity and risk analysis regarding the prices of green hydrogen, methane (natural gas), and carbon dioxide taxes.
- Do a life cycle assessment (LCA) that will represent the carbon footprint of the process.

3. Student's role in the company

3.1. Description of the company

Messer was founded in 1898 and today is the largest family-run specialist for industrial, medical and specialty gases worldwide. Under the brand 'Messer - Gases for Life' (Figure 13) the company offers products and services in Europe, Asia and the Americas.

Figure 13. Brand 'Messer - Gases for Life'.

Messer has a very diverse product portfolios on the market, it produces industrial gases such as oxygen, nitrogen, argon, carbon dioxide, hydrogen, helium, shielding gases for welding, specialty gases, medical gases and many different gas mixtures.

Messer has state-of-the-art research and competence centres in which it develops applied technologies for the use of gases in almost every sector of industry, in food technology and environmental technology, medicine as well as research and science. Messer is committed to the education and training of talented young professionals, who represent an important investment in the competitiveness and capability of the company.

Messer Ibérica is part of the Messer Industries (Figure 14) and it has been operating since 1970 in the Tarragona petrochemical complex, the largest in southern Europe, where it has air separation units and supplies gases through its own network of gas pipelines.

It has gas liquefaction and packaging plants in Tarragona and Alicante. It markets all its products directly and through a wide network of distributors that covers the entire Iberian Peninsula.

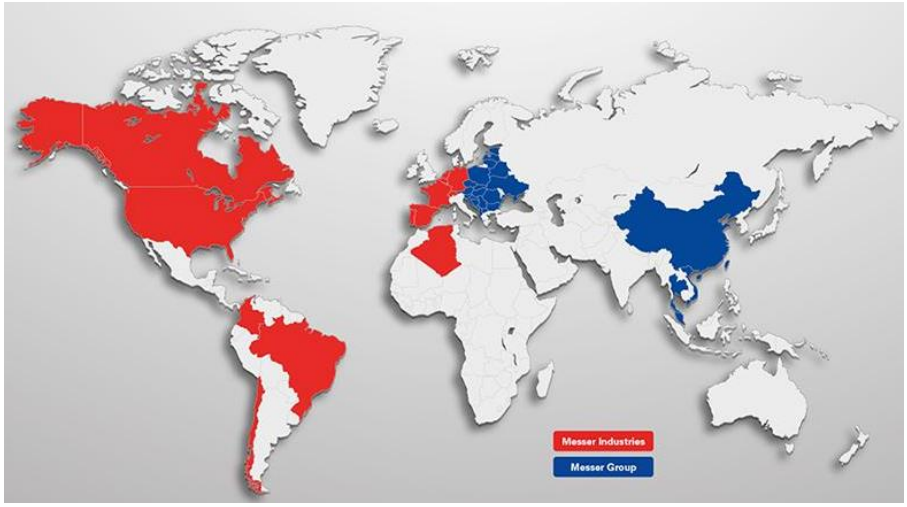

Figure 14. Messer Group acquired the majority of Linde AG's gases business in North America and certain Linde and Praxair business activities in South America in 2019 in a joint venture – called Messer Industries GmbH with CVC Capital Partners. Data source from https://corporate.messergroup.com/.

3.2. Goals and products

3.2.1. Messer's mission statement

As an owner-managed family business, Messer Group, Messer Industries and Messer Ibérica are focused on the future whilst considering the different conditions in the existing markets. Through entrepreneurial flair, farsighted thinking and continuous improvement, they create added value for their customers and so, secure mutual success in the long term.

3.2.2. Messer's values

- Customer orientation: Messer is focused on the individual requirements of their customers and they help improve their competitiveness and performance.
- Employee orientation: Messer trains, develops and promotes motivated and efficient employees with integrity.
- Responsible behaviour: Messer takes social responsibilities towards society.
- Corporate responsibility.
- Excellence: Messer's actions are based on technical expertise, innovation and flexibility.
- Mutual trust and respect.

3.2.3. Products and services

Messer manufactures and supplies oxygen, nitrogen, argon, carbon dioxide, hydrogen, helium, shielding gases for welding, specialty gases, medical gases and food gases as well as many different gas mixtures.

- Technical gases: ferroline gases (for plain and low-alloy steels), inoxline gases (for high-allow steels), aluline gases (for aluminium and non-ferrous metals) and addline (for additive manufacturing of metals).
- Specialty gases: high purity gases, noble gases, liquid helium and standard mixtures.
- Gases for the food industry: gourmet C (carbon dioxide), gourmet N (nitrogen), gourmet O (oxygen), gourmet A (argon) and gourmet mixtures with different compositions.

Apart from that, Messer also offers cutting edge solutions for the metal-working industry through "Messer cutting systems". Its main services are oxyfuel technologies and metal processing facilities.

3.3. Internship

The student develops their tasks within the company Messer Ibérica de Gases that has the following organization chart (Figure 15).

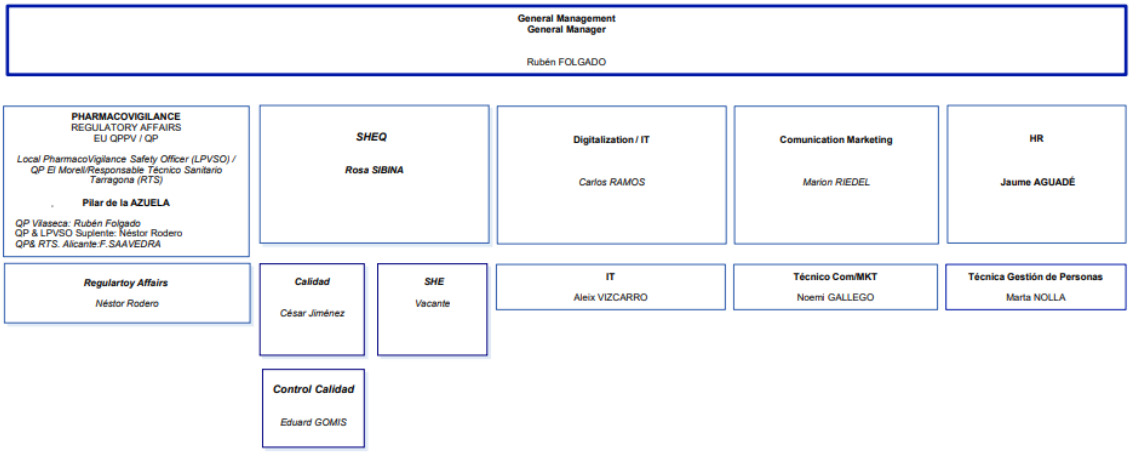

Figure 15. Organization chart of Messer Ibérica de Gases.

The student is located in the Vilaseca site in the sales department of the company with Enric Acosta as manager. Specifically, within the area of bulk supply and gas applications as shown in Figure 16. The main role of the student is to accelerate the know-how of the company on hydrogen applications (e.g., combustion and fuel cells for transportation).

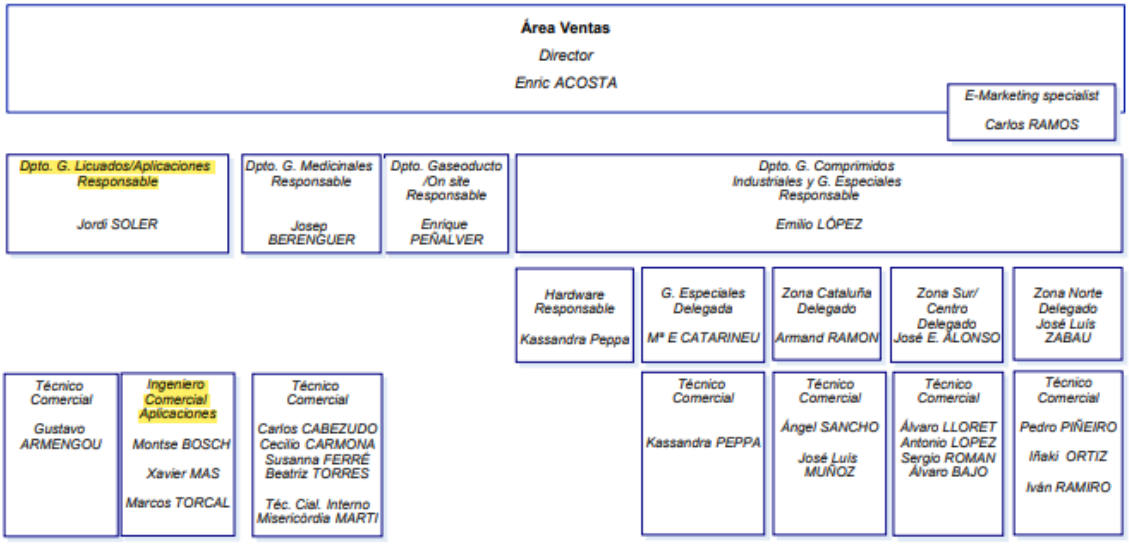

Figure 16. Organization chart of the sales department.

The main tasks are:

- Develop a new thermodynamic model for a furnace fuelled with hydrogen-enriched methane, using Microsoft Excel©.
- Develop a new thermodynamic model for a boiler fuelled with hydrogen-enriched methane, using Microsoft Excel© and Aspen EDR©.
- Carry out a market study of hydrogen, identify potential competitors for Messer Ibérica, find new projects related to hydrogen in Spain (*tenders*) and perform a benchmarking of the current automobile sector in Spain.
- Life cycle assessment (LCA) of an eco-plant of hydrogen production.

Table 2 shows a Gantt chart with all four tasks that the student accomplishes during the internship.

Table 2. Gantt chart.

Tasks\Weeks	1	2	3	4	5	6	7	8	9	10	11	12	13	14	15	16	17	18	19	20	21	22	23	24
Furnace TM																								
Boiler TM																								
Market study																								
LCA																								

These tasks, eventually, will lead to the development of the project: "Techno-economic assessment of a hydrogen-enriched boiler of 44 MW-thermal power". This project was born because of the need of decarbonizing the current society. Messer Ibérica is part of the consortium that will collaborate in the design and construction of the largest electrolyser in Spain and whose commissioning is expected in 2025 (Government of Catalonia, 2022). The core values of the company also lead to the growth of the company. Messer Ibérica will build a new ASU (air separation unit) in Vilaseca with a distillation column of 72 meters, which will be launched in 2023 (Government of Spain, 2020).

3.3.1. Furnace. Thermodynamic model

This task consists of developing a novel simplified thermodynamic model of a furnace fuelled with hydrogen-enriched methane. This model will substitute simulations with Computational Fluid Dynamics software. Within the gas applications department of the company, the student participates in two meetings with Xavier Mas, Jordi Soler and Dr. Martin Demuth (PhD from Messer Austria) to set out ideas and updates on the aforementioned model.

This model will be based on previous experimentation from Dr. Martin Demuth, however, since it is a novel model, the student gathers information about heat transfer, specifically about radiation and the weighted sum of grey gases model. Furthermore, the student proposes new approaches of calculation (e.g., solving the model as an optimization problem) and modelling to accomplish this task. Also, online meetings with experts in this matter such as Dr. Martin Demuth are of vital importance.

Ultimately, the development of this thermodynamic model will consist of:

- Comparison between air/methane and oxygen/methane combustion.
    - Thermodynamic calculations to assess the differences between both combustions.
- Environmental analysis of using oxygen-enhanced combustion.
    - Determination of the amount of GHG emission during the combustion process via spreadsheets.
- Evaluation of furnace efficiency using oxygen-enhanced and oxy-fuel combustion.
    - Development of heat transfer (convection and thermal radiation) calculations in a furnace.
    - Thermodynamic study of the heat capacities of all gases involved in the process at different temperatures.
    - Use of the weighted sum of grey gases model to study the thermal radiation inside the furnace.

- Comparison between methane, hydrogen and hydrogen-enriched methane (HEM) combustion.
    - Thermodynamic calculations to assess the differences between both combustions.

3.3.2. Boiler. Thermodynamic model

This task consists of developing a novel simplified thermodynamic model of a water-tube boiler fuelled with hydrogen-enriched methane. This model will substitute simulations with Computational Fluid Dynamics software. Within the gas applications department of the company, the student participates in three meetings with Xavier Mas, Jordi Soler and Dr. Martin Demuth (PhD from Messer Austria) to set out ideas and updates on the aforementioned model.

Ultimately, the development of this thermodynamic model will consist of:

- Evaluation of water-tube boiler efficiency using HEM combustion.
    - Heat transfer (convection and thermal radiation) calculations in a water-tube boiler.
    - Use of the weighted sum of grey gases model to study the thermal radiation inside the boiler.
    - Usage of simulation tools like Aspen© to simulate a gas fired heater and guarantee the accuracy of the simplified model.

3.3.3. Market study

This task is carried out within the sales department and consists of performing an analysis of the current prices of grey, blue and green hydrogen. Moreover, the student gathers information on future projections of gas natural prices, hydrogen prices and carbon taxes. Having an expert idea of the future market of hydrogen is vital for the strategy of Messer Ibérica.

Thereby, the student participates in monthly meetings with Xavier Mas, Jordi Soler and Rubén Folgado (general manager of Messer Ibérica) to set out updates on this matter.

The student also identifies new *tenders* from the Spanish government and carries out a benchmarking of the current automobile sector (cars and lorries). This benchmarking consists of:

- A market study of the car and lorry sector. Which brands have the greatest market share according to the fuel used.
- Fuel consumption of vehicles powered by diesel, electricity and hydrogen.

These investigations are the result of the objectives of the company, these are, to focus on the future whilst considering the different conditions in the existing markets and consider the individual requirements of their customers and, ultimately, society.

3.3.4. Life cycle assessment of an eco-plant

This task is carried out within the gas applications department (which is within the sales department of the company) and consists of performing a carbon footprint analysis of an eco-plant that produces hydrogen. The carbon footprint analysis is performed under the ISO 14067:2018 in collaboration with Marcos Torcal and Thierry Laure (environmental specialist from Enerkem).

4. Methodology

A techno-economic assessment (TEA) is often carried out on new technologies that are designed for environmental purposes (Kuppens et al., 2015). The diversity of these technologies studied by a TEA is illustrated by examples such as recycling practices of polymers (Larrain et al., 2021), coal gasification processes with and without CO_2 capture (Man et al., 2014), hydrogen production methods (Yukesh Kannah et al., 2021), among many others. Analysis of these examples shows that any good TEA must have a clear mass and energy balances, and next the economic feasibility is explored which can provide information for decision making.

Linking technical with economic aspects of a hydrogen-enriched water-tube boiler is essential to design effective products and pricing, for this purpose, TEAs are a useful tool. This method directly translates an alteration in a technological parameter into an economic indicator.

Following the TEA steps as presented in the cited literature (Thomassen et al., 2019), first a market study is performed to analyse the potential process prices. Afterwards, mass and energy balances of the water-tube boiler are carried out with a technological assessment. Then, to calculate the operational cost and other indicators, an economic assessment is carried out. Also, the change on the operational cost is studied with a sensitivity analysis after varying the input variables and with a risk analysis the ranges of the overall cost are thoroughly examined. Finally, an environmental impact study that will represent the carbon footprint of the process is carried out.

The present study focuses on the TEA of a hydrogen-enriched boiler of 44 MW of thermal power. The characteristics and dimensions of the boiler are found in Chapter 2.

4.1. Market study

The cost of the process is mainly linked to the price of the available fuel and oxidizer. In this case, mainly the price of natural gas, electricity and hydrogen. Values of natural gas, electricity and hydrogen prices are collected from databases.

The price of electricity in the European Union (EU) depends on a range of different supply and demand conditions, including the geopolitical situation, the national energy mix, import diversification, network costs, environmental protection costs, severe weather conditions, or levels of excise and taxation (Wachtmeister et al., 2018). Since most EU members have a natural gas-energy mix dependency, their electricity price is regulated mainly by gas pricing.

Gas data in Spain can be obtained from the MIBGAS (Mercado Ibérico del Gas) database and the OMIP (a regulated market operator) database, and energy prices can also be obtained from the OMIP database.

The International Energy Agency (IEA) presents forecasts of natural gas and hydrogen prices projection in several scenarios: the current state scenario, the sustainable development scenario (SDS) and the Net Zero Emissions (NZE) by 2050 (International Energy Agency (IEA), 2021).

The current state scenario projects steadily increasing prices of oil and gas, the SDS projects energy prices, considering that Paris Agreement targets are met and that there is a decarbonization of the electric matrix and a decrease in oil and gas demand, and the NZE by 2050 projects energy prices, considering that there will be zero carbon emissions by 2050.

Future projections provide credible outcomes, nonetheless, they must be treated with caution and never like an unmistakeable picture of the future.

4.2. Mass and energy balances

The input flows and output flows of the process are calculated to constitute the mass balance. The flows that enter the process are fuel, oxidizer and water. As output flows, exhaust gas and steam. It is assumed that the entering gases are dry and neither ashes nor coke are formed.

The total energy is the sum of the energy generated by the combustion reaction and the energy carried by the input gases. This must be equal to the energy supplied to the thermal load, the wall losses and that carried away by the flue gas. A couple of approaches are used to calculate the mass and energy balance of the process in order to guarantee the accuracy of the results:

- A simplified thermodynamic model of a boiler.
- An Aspen Exchanger Design and Rating (EDR)© simulation.

4.2.1. Simplified thermodynamic model

Accurate determination of the performance of a boiler (steam generator) requires significant expenditure of time and money. Many measurements are required to account for all losses, especially in the determination of efficiency by the energy balance method. Therefore, to avoid this expenditure of time and money, a simplified thermodynamic model is defined.

(Mayr et al., 2018) developed a zero/one dimensional thermodynamic model to determine the influence of oxygen-enriched combustion on the heat transfer, gas and wall temperatures in a furnace. The model was determined to be very time efficient and hence was used in Microsoft Excel©, furthermore, the model showed great agreement with the measurements and the CFD simulations. Thereby, this model will be used to study the influence of HEM in a water-tube boiler.

4.2.1.1. Water-tube boiler model

The simplified model consists of an energy balance. Firstly, the system boundaries for the thermodynamic system must be defined. For this system, the boundaries were defined at the outer walls of the firebox insulation. On the system, the different input and output heat flows are balanced, as shown in Figure 17.

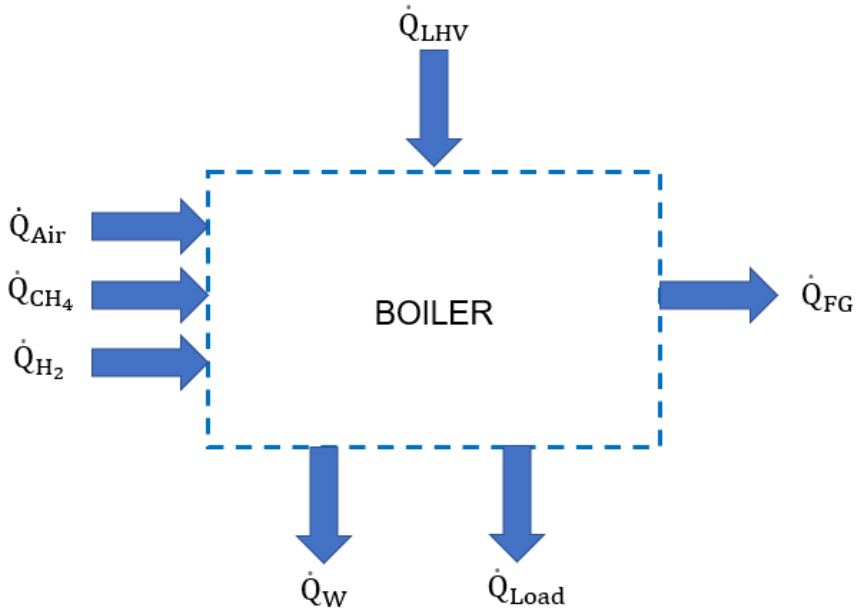

Figure 17. Energy balance of the boiler.

The following heat flows are fed into the thermodynamic system: the heat flow of the combustion air ($\dot{Q}_{Air}$), the heat flow of methane ($\dot{Q}_{CH_4}$), the heat flow of hydrogen ($\dot{Q}_{H_2}$) and the release of the chemical energy of the fuel, which is represented by the LHV ($\dot{Q}_{LHV}$). The system's output heat flows are the heat flow of the flue gas ($\dot{Q}_{FG}$), the heat losses through the walls ($\dot{Q}_W$), and the heat flow to the thermal load, namely, the tubes with containing water ($\dot{Q}_{Load}$). The energy balance of the entire boiler is then given by Equation 16.

$$0 = \dot{Q}_{Air} + \dot{Q}_{CH_4} + \dot{Q}_{H_2} + \dot{Q}_{LHV} - \dot{Q}_{FG} - \dot{Q}_W - \dot{Q}_{Load} \quad \text{Equation 16}$$

The variables in Equation 16 are defined as follows:

$$\dot{Q}_{Air} = \dot{m}_{Air} \cdot \bar{C}_{p,Air}|_{T_{ref}}^{T_{Air}} \cdot T_{Air} \quad \text{Equation 17}$$

$$\dot{Q}_{CH_4} = \dot{m}_{CH_4} \cdot \bar{C}_{p,CH_4}|_{T_{ref}}^{T_{CH_4}} \cdot T_{CH_4} \quad \text{Equation 18}$$

$$\dot{Q}_{H_2} = \dot{m}_{H_2} \cdot \bar{C}_{p,H_2}|_{T_{ref}}^{T_{H_2}} \cdot T_{H_2} \quad \text{Equation 19}$$

$$\dot{Q}_{LHV} = \dot{m}_{CH_4} \cdot LHV_{CH_4} + \dot{m}_{H_2} \cdot LHV_{H_2} \quad \text{Equation 20}$$

$$\dot{Q}_{FG} = \dot{m}_{FG} \cdot \bar{C}_{p,FG}|_{T_{ref}}^{T_{FG}} \cdot T_{FG} \quad \text{Equation 21}$$

The mass flow of the combustion air ($\dot{m}_{Air}$), the mass flows of the fuel methane ($\dot{m}_{CH_4}$) and fuel hydrogen ($\dot{m}_{H_2}$) are known parameters. The temperatures of the different mass flows (T_{Air}, T_{CH_4} and T_{H_2}) are also known parameters, and the temperature reference (T_{ref}) is 0ºC. The variable LHV_{CH_4} stands for the lower heating value of methane, with a value of 50.00 MJ/kg and the variable LHV_{H_2} stands for the lower heating value of hydrogen, with a value of 120.00 MJ/kg.

The specific heat capacities of each compound are needed at different temperatures. A polynomial of degree two is used to fit the existing data found on the Aspen© database (ideal gas heat capacity coefficients or CPIG) for each compound.

Equation 22 shows the fitting polynomial for the specific heat capacity of different compounds and Table 3 shows the coefficients for all compounds present in the energy balance. Where MW_i is the molecular weight of compound *i.*

$$\bar{C}_{p,i}|_{T_{ref}}^{T}\left[\frac{kJ}{kg\cdot K}\right]=\frac{[C_1+C_2\cdot T+C_3\cdot T^2]}{MW_i}\quad \text{where T is in °C} \qquad \text{Equation 22}$$

Table 3. Coefficient values for different compounds.

Coeff.	Methane	Oxygen	Nitrogen	Carbon dioxide	Water	Hydrogen
C_3	-1.351E-05	-1.979E-06	-1.509E-06	-5.691E-06	-2.281E-06	-1.730E-07
C_2	0.0606	0.00814	0.00706	0.0225	0.0149	0.00333
C_1	34.568	29.584	28.313	39.807	32.018	28.298

These values were found using the *polyfit* formula extension available in MATLAB© (academic license). The code is available at Section A of the Appendix, along with the used data.

Note that the specific heat capacity of air ($\bar{C}_{p,Air}|_{T_{ref}}^{T_{Air}}$) will be the weighted sum of oxygen and nitrogen and the specific heat capacity of flue gas ($\bar{C}_{p,FG}|_{T_{ref}}^{T_{FG}}$) will be the weighted sum of oxygen, nitrogen, carbon dioxide and water vapor.

The mass flow of flue gas ($\dot{m}_{FG}$) and the specific heat capacity ($\bar{C}_{p,FG}|_{T_{ref}}^{T_{FG}}$) are not known and must be determined. In order to calculate these values, the gas composition of the flue gas must be known. For the calculation of the flue gas composition, the fuel is assumed to be completely combusted. In Equation 23, the chemical equation for the combustion of methane for different oxidizers and oxidizer-fuel equivalence ratios (λ) is given. And in Equation 24, the chemical equation for the combustion of hydrogen is given.

$$CH_4+2\lambda\left(O_2+\frac{\theta_{N_2,oxi}}{\theta_{O_2,oxi}}N_2\right)\rightarrow CO_2+2H_2O+2(\lambda-1)O_2+2\lambda\frac{\theta_{N_2,oxi}}{\theta_{O_2,oxi}}N_2 \qquad \text{Equation 23}$$

$$2H_2+\lambda\left(O_2+\frac{\theta_{N_2,oxi}}{\theta_{O_2,oxi}}N_2\right)\rightarrow 2H_2O+(\lambda-1)O_2+\lambda\frac{\theta_{N_2,oxi}}{\theta_{O_2,oxi}}N_2 \qquad \text{Equation 24}$$

The oxidizer is assumed to be a mixture of oxygen ($\theta_{O_2,oxi}$ volume fraction of oxygen in the oxidizer equal to 0.21) and nitrogen ($\theta_{N_2,oxi}$ volume fraction of nitrogen in the oxidizer equal to 0.79). And a 10% excess of oxidizer is assumed.

All variables of the energy balance (Equation 16) have now been defined except for $\dot{Q}_W$ and $\dot{Q}_{Load}$.

The heat flow through the wall ($\dot{Q}_W$) and the thermal load ($\dot{Q}_{Load}$) in the boiler are calculated by an approach proposed by (Jaklič et al., 2007). However, in this case, the wall temperature is not an input parameter. In this model, the wall temperature is obtained via thermodynamic calculations.

(Jaklič et al., 2007) used the correlations by (Hottel H.C., 1969) to calculate the absorption and the emissivity coefficients of the flue gas, where this model uses the weighted sum of grey gases model (WSGGM) with the coefficient proposed by (Smith T. F. et al., 1982) to calculate these values.

Figure 18 depicts a schematic drawing of the heat transfer in the boiler.

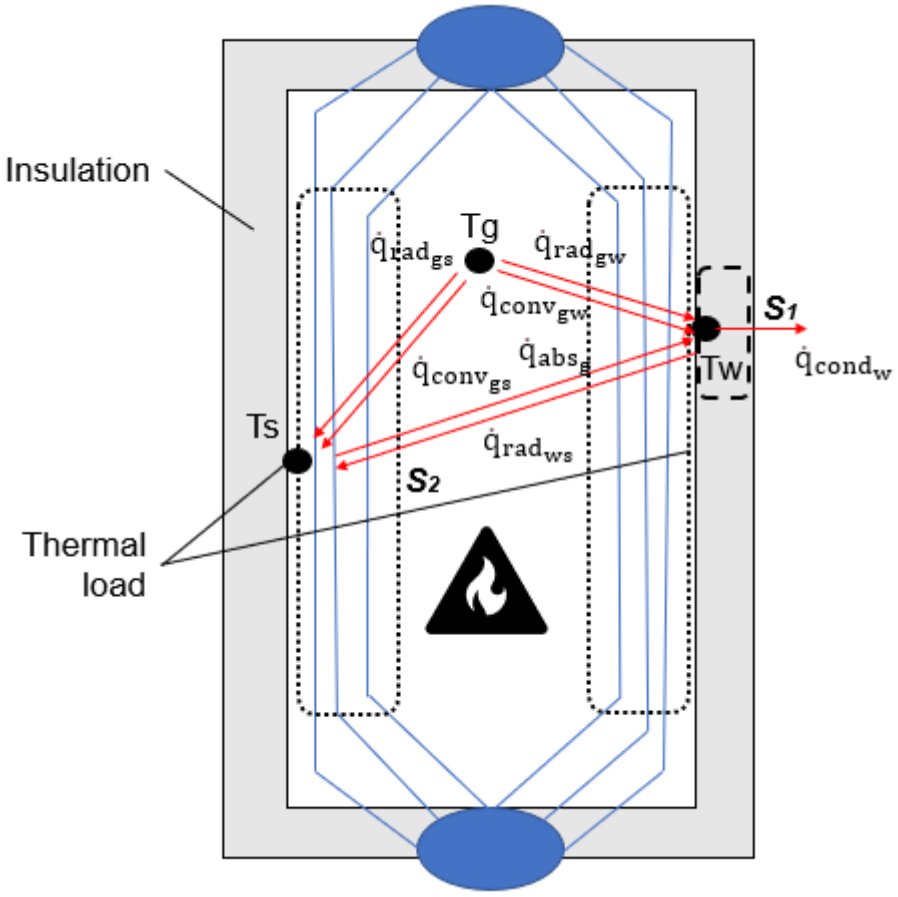

Figure 18. Heat transfer inside the boiler. Adapted from (Mayr et al., 2018).

The boiler is divided into two thermodynamic systems (S_1 and S_2), which interact with each other. The thermodynamic system S_1 balances the heat flows at the wall, and the thermodynamic system S_2 balances the heat flows to the thermal load inside the boiler. The heat flow between the gas phase and the wall is transferred both convectively and radiatively. This is also the case for the heat flow between the gas phase and the thermal load. The heat flow between the wall and the thermal load is transferred via thermal radiation of grey surfaces and is reduced by the amount of radiation the gas phase can absorb. For each thermodynamic system, an energy balance can be attained. Equation 25 shows the energy balance for S_1.

$$0 = \dot{q}_{rad_{gw}} \cdot A_w + \dot{q}_{conv_{gw}} \cdot A_w - \dot{q}_{cond_w} \cdot A_w - \dot{q}_{rad_{ws}} \cdot A_s + \dot{q}_{abs_g} \cdot A_s \quad \text{Equation 25}$$

The variables in Equation 25 are defined herein:

$$\dot{q}_{rad_{gw}} = \varepsilon_g(T_g) \cdot \sigma \cdot {T_g}^4 - \alpha_g(T_g, T_w) \cdot \sigma \cdot {T_w}^4 \quad \text{Equation 26}$$

$$\dot{q}_{conv_{gw}} = h_{gw} \cdot (T_g - T_w) \quad \text{Equation 27}$$

$$\dot{q}_{cond_w} = \frac{\lambda_w}{l_w} \cdot (T_w - T_{out}) \quad \text{Equation 28}$$

$$\dot{q}_{rad_{ws}} = \frac{\varepsilon_w \cdot \sigma \cdot {T_w}^4 - \varepsilon_s \cdot \sigma \cdot {T_s}^4}{\frac{1}{\varepsilon_s} + \frac{A_s}{A_w}\left(\frac{1}{\varepsilon_w} - 1\right)} \quad \text{Equation 29}$$

$$\dot{q}_{abs_g} = \varepsilon_g(T_w) \cdot \sigma \cdot {T_w}^4 - \alpha_g(T_w, T_s) \cdot \sigma \cdot {T_s}^4 \quad \text{Equation 30}$$

Where $\dot{q}_{rad_{gw}}$ stands for the transferred radiative heat flux between gas and wall and $\dot{q}_{rad_{ws}}$ for the radiative heat flux transferred between wall and thermal load; $\dot{q}_{conv_{gw}}$ stands for the convective heat flux between gas and wall and $\dot{q}_{abs_g}$ for the absorbed heat flux by the flue gas. Finally, $\dot{q}_{cond_w}$ stands for the heat flux conducted through the insulation wall. The total surface area of the wall is represented by A_w, and the total surface area of the thermal load is represented by A_s.

Equation 26 is a simplification of the transferred radiative heat flux between the gas and wall, considering that the wall is a black surface, and calculated by the Stefan-Boltzmann law.

Equation 29 is also calculated by the Stefan-Boltzmann law. The Stefan-Boltzmann law states that the radiative heat flux emitted by a black body is proportional to the fourth power of the black body temperature ($\sigma \cdot T^4$). Real materials only emit and absorb a fraction of a black body. This is considered by the emissivity coefficient. For Equation 29 a fixed value (see Section 4.2.2) is used for the emissivity (ε_w and ε_s). The emissivity (ε_g) and the absorptivity (α_g) of the gas phase are calculated with the WSGGM and the coefficients from (Smith T. F. et al., 1982). The heat losses through the boiler walls due to conduction ($\dot{Q}_W$) are calculated using Fourier's law, Equation 28, where λ_w is the thermal conductivity of the firebox walls of the boiler, l_w is the wall thickness of the firebox and T_{out} is the temperature of the outside walls and is assumed to be at the same temperature as the atmosphere.

The convective heat flux to the wall from the flue gas is calculated using Newton's law of cooling, Equation 27, where h_{gw} is the convective heat transfer coefficient. The convective heat transfer in high temperature boilers is only minor, as most of the heat flux is transferred by thermal radiation. Therefore, the convective heat transfer coefficient was assumed to be 12 W/m^2·K.

Equation 31 shows the energy balance of S_2 (thermodynamic system for the thermal load).

$$\dot{Q}_{Load} = \dot{q}_{rad_{gs}} \cdot A_s + \dot{q}_{conv_{gs}} \cdot A_s + \dot{q}_{rad_{ws}} \cdot A_s - \dot{q}_{abs_g} \cdot A_s \quad \text{Equation 31}$$

The variables $\dot{q}_{rad_{gs}}$ and $\dot{q}_{conv_{gs}}$ are the radiative and convective heat flux from the gas to the load, and are defined herein:

$$\dot{q}_{rad_{gs}} = \varepsilon_g(T_g) \cdot \sigma \cdot {T_g}^4 - \alpha_g(T_g, T_s) \cdot \sigma \cdot {T_s}^4 \quad \text{Equation 32}$$

$$\dot{q}_{conv_{gs}} = h_{gs} \cdot (T_g - T_s) \quad \text{Equation 33}$$

Equation 32 is a simplification, considering that the thermal load is a black surface.

Moreover, it is assumed that the water inside the tubes and the tubes themselves are at the same temperature, namely, thermal conductivity is infinity for the thermal load. However, the stream properties and phase composition of fluid within the tubes is beyond the scope of this simplified model and data values from the Aspen EDR© simulation will be needed to calculate the amount of steam generated. The total steam flow within the tubes will be assessed as follows:

$$\dot{m}_{steam} = \frac{\dot{Q}_{Air} + \dot{Q}_{CH_4} + \dot{Q}_{H_2} + \dot{Q}_{LHV} - \dot{Q}_{FG}}{(H - h)} \quad \text{Equation 34}$$

Where the available heat ($\dot{Q}_{Air} + \dot{Q}_{CH_4} + \dot{Q}_{H_2} + \dot{Q}_{LHV} - \dot{Q}_{FG}$), the enthalpy of the output fluid (H) and the enthalpy of feed water (h) are used to estimate the total quantity of steam in the output stream. The vapor mass fraction from the Aspen EDR© simulation will be used to compute both H and h. Equation 35 shows the combustion efficiency.

$$\eta\,(\%) = \frac{\dot{Q}_{Load} + \dot{Q}_W}{\dot{Q}_{LHV}} \cdot 100 = \frac{\dot{Q}_{Air} + \dot{Q}_{CH_4} + \dot{Q}_{H_2} + \dot{Q}_{LHV} - \dot{Q}_{FG}}{\dot{Q}_{LHV}} \cdot 100 \quad \text{Equation 35}$$

Due to the mutual dependency of the different thermodynamic systems (entire boiler, S_1 and S_2) the calculations must be performed iteratively. The energy balance of the boiler is treated as an optimization problem, hence, the best solution among a set of many feasible solutions by efficient numerical methods needs to be found. The optimization problem is defined as follows:

$$\min\ f(T_g, T_w) = \dot{Q}_{Air} + \dot{Q}_{CH_4} + \dot{Q}_{H_2} + \dot{Q}_{LHV} - \dot{Q}_{FG} - \dot{Q}_W - \dot{Q}_{Load} \quad \text{Equation 36}$$

$$\text{s.t.}\ \dot{q}_{rad_{gw}} \cdot A_w + \dot{q}_{conv_{gw}} \cdot A_w - \dot{q}_{cond_w} \cdot A_w - \dot{q}_{rad_{ws}} \cdot A_s + \dot{q}_{abs_g} \cdot A_s = 0 \quad \text{Equation 37}$$

$$\text{s.t.}\ \dot{Q}_{Air} + \dot{Q}_{CH_4} + \dot{Q}_{H_2} + \dot{Q}_{LHV} - \dot{Q}_{FG} - \dot{Q}_W - \dot{Q}_{Load} \geq 0 \quad \text{Equation 38}$$

$$\text{s.t.}\ T_g, T_w \geq 0 \quad \text{Equation 39}$$

$$\text{s.t.}\ T_g, T_w \in R^n \quad \text{Equation 40}$$

Here the decision variables are the flue gas temperature (T_g) and the inside wall temperature (T_w). The GRG Nonlinear Solving method available in the Solver program of Microsoft Excel© is used to find the best feasible solution.

The GRG Nonlinear Solving method uses the Generalized Reduced Gradient method as implemented in Lasdon and Waren's GRG2 code (Optimizer, 1981). The GRG method can be viewed as a nonlinear extension of the Simplex method, which selects a basis, determines a search direction and performs a line search on each major iteration.

4.2.2. Aspen EDR© simulation

The process model was developed in Aspen EDR© V11. Aspen EDR© enables the user to simulate and optimize processes using modelling tools.

A fired heater model of 6000 mm of inner diameter and 18000 mm height consisting of just a firebox, without convection banks, was used to simulate the overall process. A forced draught standard burner was selected with 500 mm diameter.

A total of 40 vertical tubes were selected with a 90 mm diameter which account for a total surface area of 538.7 m^2. In this simulation a total mass flow of 16 kg/s of water was selected with an input temperature of 25ºC, an input pressure of 15 bar and zero fouling resistance. And a 10% excess of oxidizer is assumed.

The B-JAC physical properties package was used to calculate the vapor-liquid equilibria of water along the tubes.

An operation limit must be assessed, namely, the CHF, to avoid reaching a maximum value of heat transmitted and creating a film of bubbles around the tubes. Using the concept of boundary layer separation from a permeable flat plate with gas injection, (Tong, 1968) proposed a CHF correlation for subcooled flow boiling regimes:

$$\mathrm{CHF} = \mathrm{C} \cdot \frac{\mathrm{G} \cdot \mathrm{h_{fg}}}{\mathrm{Re}^{0.6}} \qquad \text{Equation 41}$$

$$\mathrm{Re} = \frac{\mathrm{G} \cdot \mathrm{D_h}}{\mu_\mathrm{f}} \qquad \text{Equation 42}$$

$$\mathrm{C} = 1.70 - 7.43 \cdot \mathrm{x_{eq}} + 12.22 \cdot \mathrm{x_{eq}}^2 \qquad \text{Equation 43}$$

The CHF is calculated via an experimental parameter (C), the mass flux (G), the heat of vaporization of water (h_{fg}) and the Reynolds number (Re). The Reynolds number is determined using the mass flux (G), the hydraulic equivalent diameter (D_h), and the fluid viscosity (μ_f).

Finally, the parameter C is computed using the steam quality (x_{eq}). And although the parameter C was determined by experimentation under pressures as high as 6.9-13.8 MPa, which are way above the operational pressure of 15 bar (1.5 MPa), the CHF value found using Equation 41 can be used as an operation limit.

Estimated CHF values are in the order of the hundreds kW/m^2; hence, it is fair to say that under the aforementioned conditions there will not be a sudden decrease in the efficiency of heat transfer.

Regarding heat transfer within the firebox, a tube-gas side heat transfer coefficient of 12 W/m^2·K was selected, a tube wall emissivity of 0.8 was assumed

and a firebox wall emissivity of 0.6 was selected. In this work, a 4-grey gas emissivity model was employed to study the radiation of the process. Finally, the calculation options of the process are presented in Table 4.

Table 4. Calculation options for a fired heater model.

Number of iterations	1000
Enthalpy relaxation factor	0.8
Pressure relaxation factor	1
Convergence criterion (temp.)	0.1 ºC
Convergence criterion (pressure)	0.1 bar

4.3. Economic assessment

The capital cost of the process will not be analysed herein since this work focuses on the economic viability of the operational process.

A baseline operating cost or blOPEX is defined (Equation 44). It represents the cost of generating 1 MJ of available heat (heat not carried away by the exhaust) with methane as fuel, and air as oxidizer with a 10% excess. For this, prices of natural gas (P_{CH_4}) and carbon tax emissions (P_{CO_2}) are needed. Note that $\dot{V}_{CH_4}$(volumetric flow of methane) and $\dot{m}_{CO_2}$ (mass flow of carbon dioxide) are in Nm^3/h and kg/h, respectively. Thus, a time conversion factor is needed (1h = 3600s).

$$\text{blOPEX}\left[\frac{€}{MJ}\right] = \frac{\dot{V}_{CH_4}\cdot P_{CH_4} + \dot{m}_{CO_2}\cdot P_{CO_2}}{3600\cdot(\dot{Q}_{Air} + \dot{Q}_{CH_4} + \dot{Q}_{H_2} + \dot{Q}_{LHV} - \dot{Q}_{FG})} \qquad \text{Equation 44}$$

The levelized cost (LC) will account for the difference of the cost of a new approach and the cost of blOPEX (Equation 45). Namely, to obtain a levelized cost that is greater than zero, the overall cost of the new approach must be higher than the overall cost of the baseline process (blOPEX). This will mean that the new approach is less economically attractive.

$$\text{LC}\left[\frac{€}{MJ}\right] = \frac{\dot{V}_{CH_4}\cdot P_{CH_4} + \dot{m}_{H_2}\cdot P_{H_2} + \dot{m}_{CO_2}\cdot P_{CO_2}}{3600\cdot(\dot{Q}_{Air} + \dot{Q}_{CH_4} + \dot{Q}_{H_2} + \dot{Q}_{LHV} - \dot{Q}_{FG})} - \text{blOPEX} \qquad \text{Equation 45}$$

If the water-tube boiler operates with methane and air, then the LC will be equal to zero. However, if cheap green hydrogen is used instead of methane, the OPEX will decrease, obtaining a LC<0.

The economic assessment will be evaluated in several scenarios, among which is a current state, the SDS and the NZE by 2050 described in 4.1.

4.4. Sensitivity analysis

A one-at-a-time sensitivity analysis is done to detect the variables that have a higher influence on the results. For this purpose, each input variable is altered independently by 10% and the output is then registered, the output being a new levelized cost. Afterwards, the sensitivity is calculated by dividing the absolute percentage change in the output variable over the percentage change in the input variable (10%).

The input variables of study are the prices of natural gas, green hydrogen, and carbon dioxide tax emissions. All other variables are assumed to not influence the overall cost of the process.

4.5. Risk analysis

The probability range of the variables is studied with a Monte Carlo simulation, using the What-If analysis add-in available in Microsoft Excel©, where the most influential variables detected with the one-at-a-time sensitivity analysis are defined as probabilistic. The probability density functions of the variables are constructed using 20,000 sampling points and a normal distribution model.

4.6. Life cycle assessment

Life cycle assessment (LCA) is a methodology for assessing environmental impacts associated with all the stages of a process or product.

Environmental impacts are changes in the natural or built environment, resulting directly from an activity, that can have adverse effects on the air, land, water, and the inhabitants of the ecosystem. Pollution, contamination, or destruction that occurs because of an action, that can have short-term or long-term ramifications is considered an environmental impact.

In this section, a LCA of a water-tube boiler of 44 MW-t power fuelled with HEM will be carried out.

The first stage of any LCA is identifying the study goal and scope and the functional unit. This study presents the results in terms of carbon footprint from cradle-to-gate in g CO_2-e/kg_{steam}, that is, mass of CO_2-equivalent emitted per mass of steam generated at 200ºC (~15 bar of vapor pressure) in a water-tube boiler of 44 MW-t power. This study uses 100-year GWP values from the Fifth Assessment Report of the Intergovernmental Panel on Climate Change (Myhre et al., 2016; Shindell et al., 2013). The scope of this LCA is exploration, extraction and distribution of conventional natural gas, combustion of natural gas and production of green hydrogen via wind energy to generate high-pressure steam. The second stage is an assessment of the inventory of the life cycle, which considers the quantification of inputs and outputs of the process. The third stage is the study of the environmental impact of each GHG emitted during the process. The fourth and last stage is the interpretation and analysis of the life cycle study.

5. Results and discussion

5.1. Market study

The cost of the process is mainly linked to the price of the available fuel.

Figure 19 shows the prices of natural gas and electricity in Spain during the period 2019-2022, furthermore, Figure 20 depicts prices of natural gas and oil in the following years based on three different scenarios: a current state that considers steadily increasing prices, Sustainable Development scenario (SDS) that assumes a decrease in prices from 2025 and Net Zero Emissions (NZE) by 2050 that considers zero emissions, globally, by the year 2050.

Current transaction prices are projected into the future according to forecasts of the International Energy Agency (International Energy Agency (IEA), 2021).

Natural gas prices in Spain during 2019-2022 were obtained from the MIBGAS and OMIP database and converted into EUR/Nm^3 of gas considering that the lower heating value of methane is 36.00 MJ/Nm^3 (Green et al., 2019). Also, electricity prices in Spain from 2019 until 2022 were obtained from the MIBGAS and OMIP database.

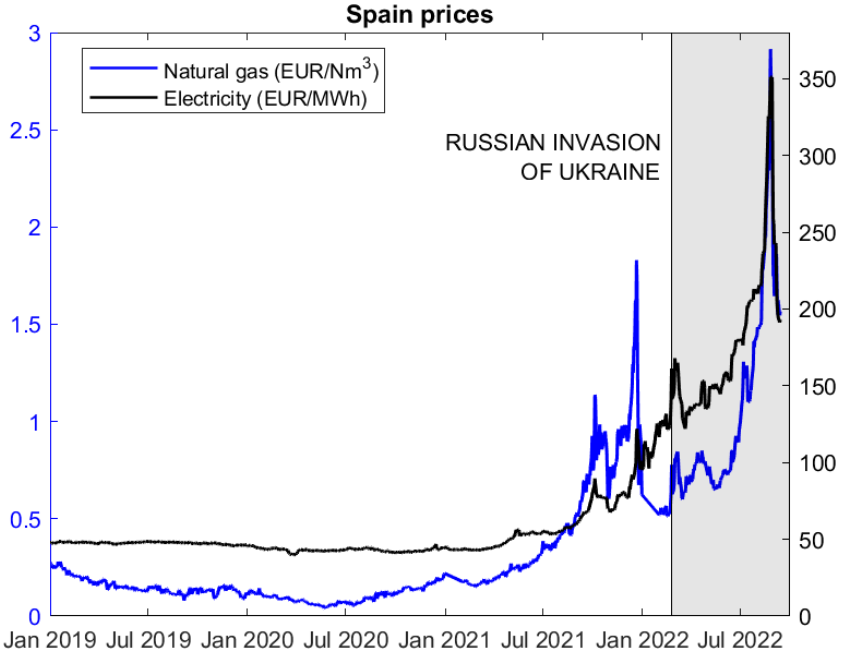

Figure 19. Gas and electricity prices in Spain (data values from 01/01/2019 to 13/09/2022). Source: MIBGAS (https://www.mibgas.es/en) and OMIP (https://www.omip.pt/en).

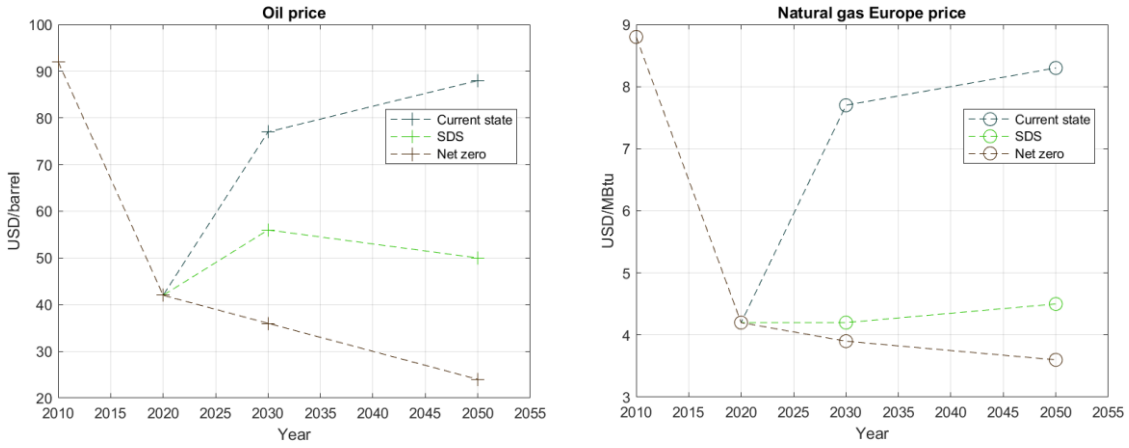

(a) (b)

Figure 20. (a) Oil prices worldwide and (b) natural gas prices in Europe. Source: IEA (International Energy Agency (IEA), 2021).

There is little confidence on future projections of green hydrogen prices (George et al., 2022; International Renewable Energy Agency, 2020), however, Figure 21 shows the current prices of grey and blue hydrogen, and future projections of prices of green hydrogen in the current state scenario, in the SDS framework and the NZE by 2050 scenario for 2030.

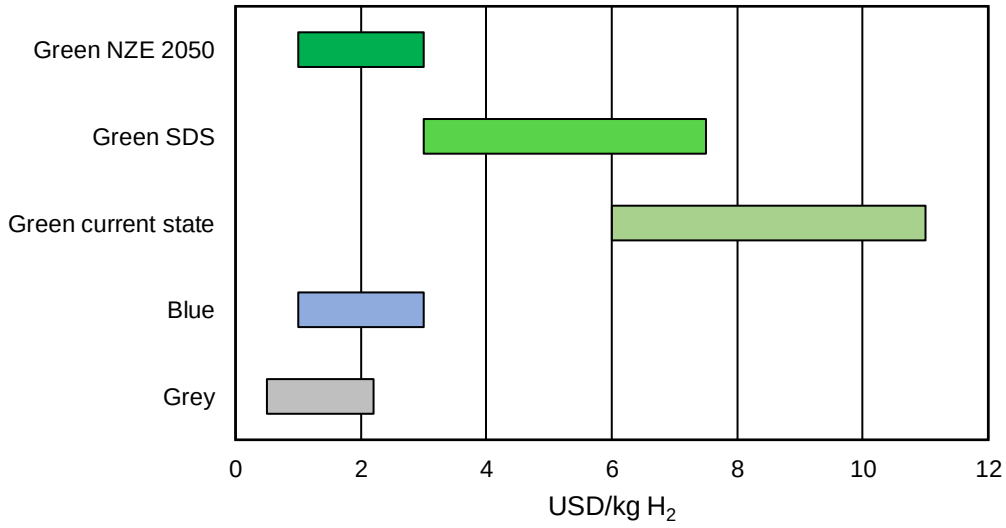

Figure 21. Levelized cost of blue and grey hydrogen in 2020, and future projections for green hydrogen in 2030. Source: IRENA and IEA (Armaroli et al., 2022; International Energy Agency, 2021), and (Newborough & Cooley, 2020).

Figure 22 depicts the carbon dioxide prices for industry and energy production in Europe, again, in three different scenarios: a current state that considers current legislations, SDS that assumes an increase in carbon dioxide taxes from 2020 and NZE by 2050 that considers zero emissions by the year 2050 and, hence, the taxation on carbon emissions increases.

Ultimately, NZE by 2050 is the most desirable case but also the most difficult to achieve because the pledges announced by most of the governments fall well short of what is required to bring global energy-related carbon dioxide emissions

to net zero by 2050 and give the world an even chance of limiting the global temperature rise to 1.5 °C (International Energy Agency (IEA), 2021).

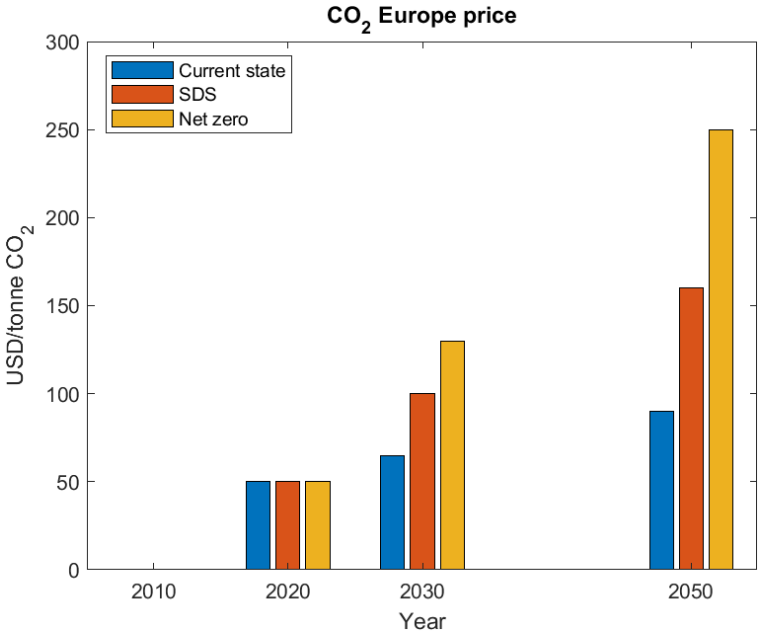

Figure 22. CO_2 prices for industry and energy production in Europe. Source: IEA (International Energy Agency (IEA), 2021).

5.2. Mass and energy balances

In this section, the models described in Chapter 4.2 are used to calculate the mass and energy balances of a water-tube boiler of 44 MW of thermal power that produces 20-30 tonne/h of high-pressure steam on average and can produce up to 75 tonne/h of steam.

The gas fired water-tube boiler that is initially fuelled with methane, is ultimately powered with hydrogen-enriched methane.

In Figure 23 the available heat as calculated by the thermodynamic model ($\dot{Q}_{\mathrm{Air}} + \dot{Q}_{\mathrm{CH_4}} + \dot{Q}_{\mathrm{H_2}} + \dot{Q}_{\mathrm{LHV}} - \dot{Q}_{\mathrm{FG}}$) is compared to the results of the Aspen EDR© simulation. Moreover, the average value is calculated and will be used later for the economic assessment. The thermodynamic model shows great agreement with the Aspen EDR© simulation.

The simplified thermodynamic model predicts an available heat flow of 22845.9 kW with 0% H_2 volume fraction (100% CH_4), and a heat flow of 24571.8 kW with 80% H_2 volume fraction (20% CH_4). The Aspen EDR© simulation predicts a heat flow of 23089.8 kW with 0% H_2 volume fraction (100% CH_4), and a heat flow of 24574.9 kW with 80% H_2 volume fraction (20% CH_4). Both calculations show the same tendency, that is, with increasing hydrogen fraction, there is a slight increase on the available heat. This work demonstrates that hydrogen-enriched methane produces less flue gas and, hence, less energy is carried out by the exhaust.

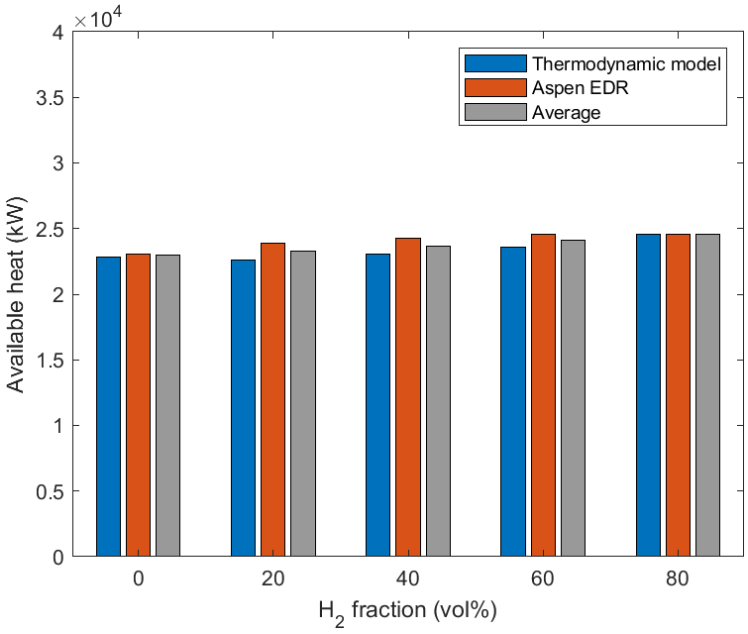

Figure 23. Comparison of the available heat calculated with the thermodynamic model and the Aspen EDR© simulation (the average value of the two calculations also appears).

In Figure 24, the flue gas temperature is calculated by the thermodynamic model and by the Aspen EDR© simulation. Also, the average value of both calculations is worked out. The gas temperature values of the Aspen EDR© simulation are flue gas temperatures leaving the radiation section.

From Figure 24 it is possible to see that the values and the trend of the exhaust gas temperatures are predicted in the same way by both the simplified model and the Aspen EDR© simulation. It shows a slight increase on the temperature of the exhaust as the hydrogen fraction in the fuel increases.

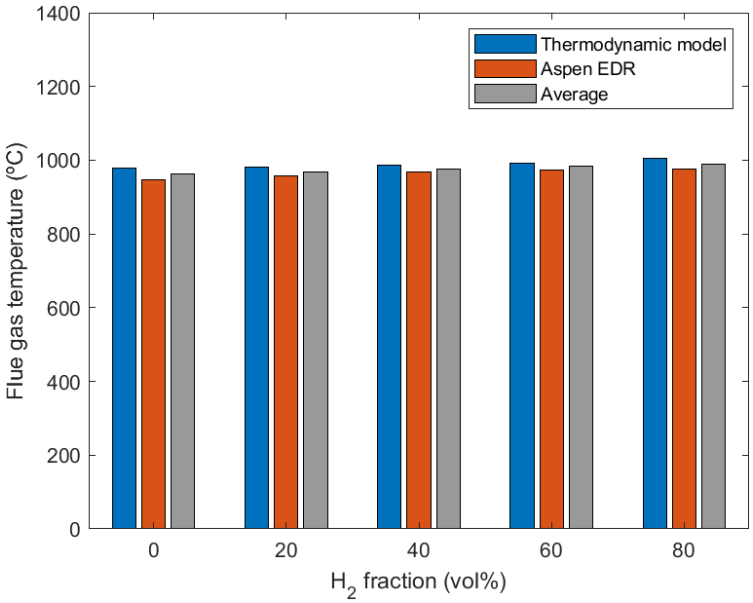

Figure 24. Comparison of the flue gas temperature calculated with the thermodynamic model and the Aspen EDR© simulation (the average value of the two calculations also appears).

In Figure 25 the combustion efficiency as calculated by the thermodynamic model is compared to the results of the Aspen EDR© simulation. Moreover, the average

value is calculated. The thermodynamic model shows great agreement with the Aspen EDR© simulation.

The simplified thermodynamic model predicts a combustion efficiency (η) of 51.92% with 0% H_2 volume fraction (100% CH_4), and a combustion efficiency of 55.85% with 80% H_2 volume fraction (20% CH_4). The Aspen EDR© simulation predicts a combustion efficiency of 52.93% with 0% H_2 volume fraction (100% CH_4), and an efficiency of 56.08% with 80% H_2 volume fraction (20% CH_4). This work shows that hydrogen-enriched methane produces less flue gas and, hence, less energy is carried out by the exhaust and, ultimately, higher efficiencies can be achieved.

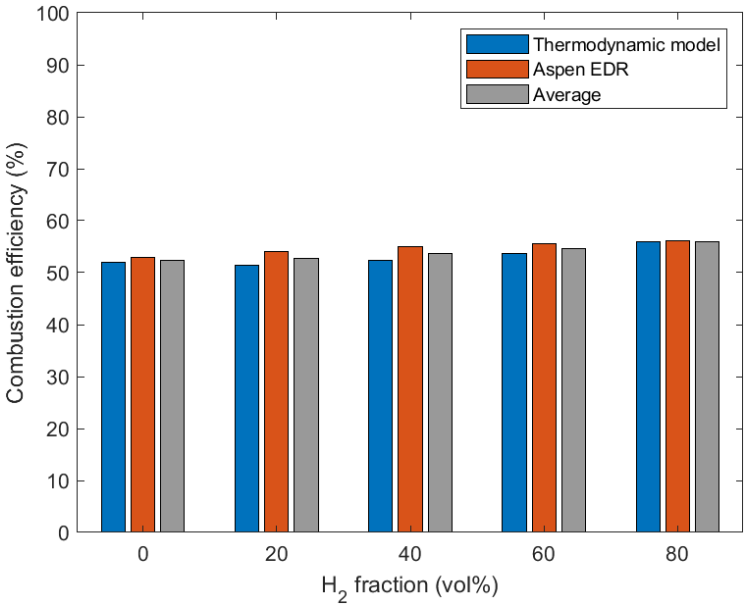

Figure 25. Comparison of the combustion efficiency calculated with the thermodynamic model and the Aspen EDR© simulation (the average value of the two calculations also appears).

In Figure 26 the steam flow at 200ºC as calculated by the thermodynamic model is compared to the results of the Aspen EDR© simulation. Moreover, the average value is calculated.

To estimate the steam flow using the simplified thermodynamic model, the vapor fraction value from the Aspen simulations was needed since the stream properties and phase composition of fluid within the tubes is not calculated with this model. Also, a P-H diagram (Section C of the Appendix) for water was employed to calculate enthalpies.

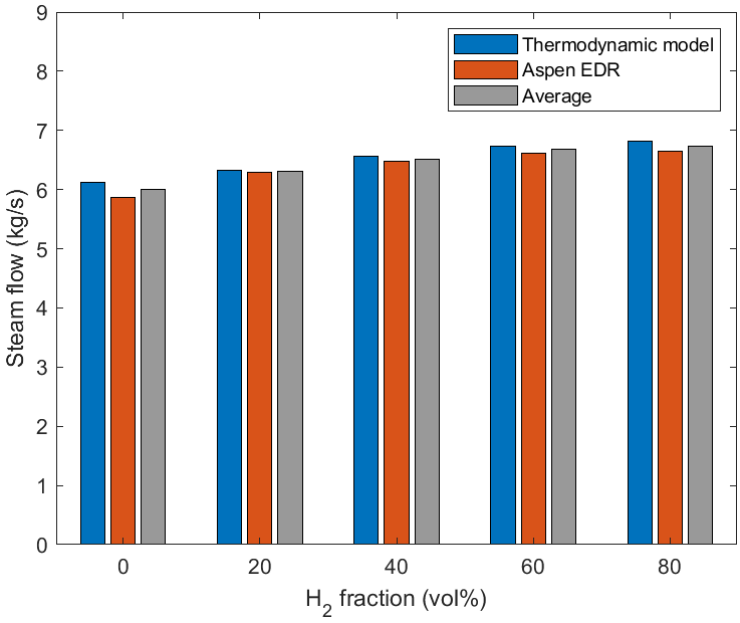

Figure 26. Comparison of the steam flow calculated with the thermodynamic model and the Aspen EDR© simulation (the average value of the two calculations also appears).

5.3. Economic assessment

A baseline operational cost or blOPEX is defined. It represents the cost of generating 1 MJ of available heat ($\dot{Q}_{Air} + \dot{Q}_{CH_4} + \dot{Q}_{H_2} + \dot{Q}_{LHV} - \dot{Q}_{FG}$) using methane as fuel, and air as oxidizer. Thus, a matrix of prices needs to be developed. Table 5 shows the matrix of prices which include the price of natural gas (average price from 01/01/2019 until 13/09/2022 in Spain) and the carbon emission tax price for 2020.

Table 5. Matrix of prices for the blOPEX. **Average price from 01/01/2019 until 13/09/2022 in Spain.*

	Methane (€/Nm^3)	**CO_2 (€/kg)**
Price	0.346*	0.050

Considering that an input of 4400 Nm^3/h of methane is needed to generate 44 MW of theoretical thermal power, and this emits roughly 8662 kg/h of CO_2; the blOPEX is 0.024 €/MJ.

The levelized cost (LC) is calculated considering this blOPEX.

Three different LC must be considered according to the projected scenarios for year 2030:

- LC for a current state scenario.
- LC for a Sustainable Development scenario (SDS).
- LC for an NZE by 2050 scenario.

Table 6 depicts a matrix of prices for these three different scenarios which include prices of gas, green hydrogen, and carbon emission taxes.

Table 6. Matrix of prices for levelized cost (LC) calculations. Data from Chapter 4.1.

2030			
	Methane (€/Nm^3)	Green H_2 (€/kg)	CO_2 (€/kg)
Current state	0.268	8.50	0.065
SDS	0.146	5.25	0.100
Net zero	0.136	2.00	0.130

Average results from Chapter 5.2 are used to estimate the levelized cost for all cases. Figure 27 depicts the corrected operational cost for three different future scenarios and different hydrogen fractions.

The corrected costs for 0% H_2 fraction are negative because the overall projected cost of the process is lower than the base-line costs or current costs. According to the forecast scenarios, the price of natural gas (methane) will decrease. Nonetheless, as the hydrogen fraction increases, so does the corrected cost of the process. Green hydrogen will be still way more expensive than current methane in two out of three scenarios: current state and SDS. NZE by 2050 is the most desirable scenario since fuel prices will decrease substantially thanks to an increase on the renewables.

However, note that future projections for 2030 state that 100% methane will be the best fuel option from an economic perspective in comparison with nowadays pricing.

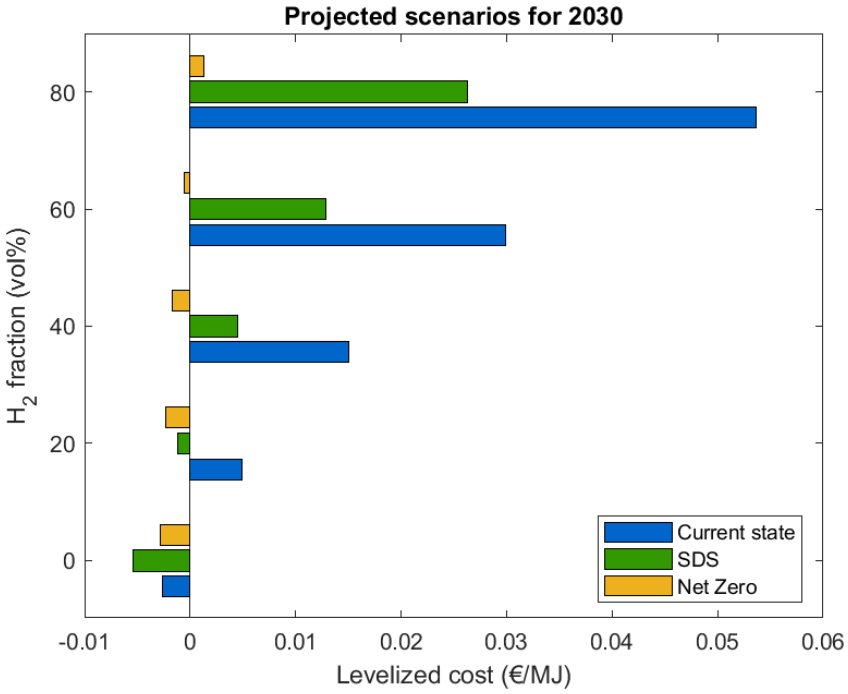

Figure 27. LC for three different projected scenarios for 2030.

5.4. Sensitivity analysis

A one-at-a-time sensitivity analysis is done to detect the variables that have a higher influence on the results. The base case model is defined in Chapter 5.3 and each variable is altered independently by 10% and the new LC is registered. The sensitivity is calculated by dividing the absolute percentage change in the output variable over the percentage change in the input variable (10%).

The one-at-a-time sensitivity analysis in Figure 28 indicates that all three input variables are important for the operational cost, but the two most important parameters are carbon dioxide tax emissions and green hydrogen price. On average, a 10% change on methane pricing generates more than 20% change on the output; a 10% change on green hydrogen pricing generates more than 30% change on the output; and a 10% change on carbon tax emission generates almost 40% output change.

Different future scenarios have strong differences on the sensitivity. For instance, 10% change on the carbon dioxide tax emission, produces nearly the same change on the output if the current state scenario is considered, but, more than 70% change on the output if NZE is considered. This is mainly because tax emission prices are very different among all three scenarios.

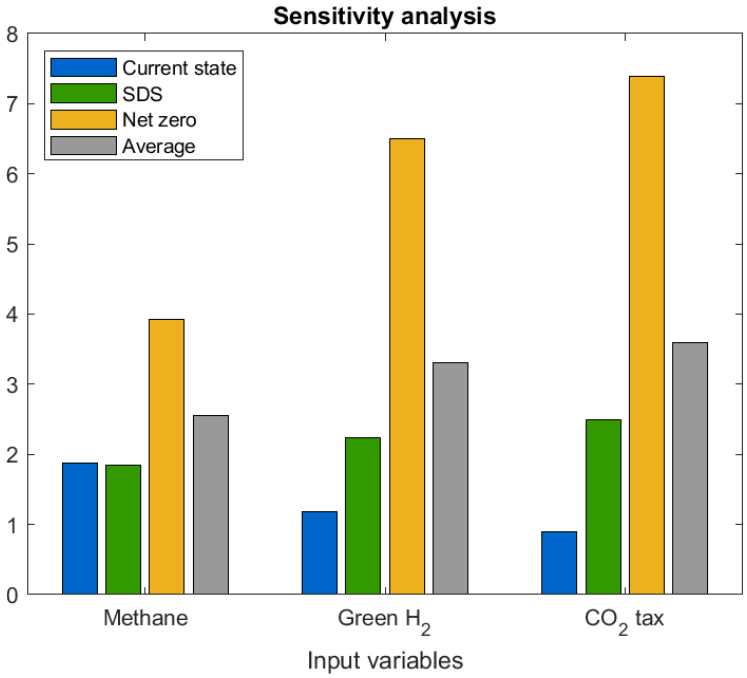

Figure 28. One-at-a-time sensitivity analysis for projected scenarios for 2030.

5.5. Risk analysis

The estimation of the operating expenses of a water-tube boiler is highly uncertain since prices depend on a range of different supply and demand conditions, including the geopolitical situation, the national energy mix, import diversification, network costs, environmental protection costs, severe weather conditions, or levels of taxation.

In accordance with the one-at-a-time sensitivity analysis results, green hydrogen price and carbon tax emissions are modelled as probabilistic variables.

Table 7 summarizes the uncertainty ranges that have been found in the literature for 2030 projections. Next, Monte Carlo simulations have been performed using the What-If analysis add-in. Risk of unsustainable economic scenarios are found using 20,000 sampling points and a normal distribution model.

Table 7. Uncertainty ranges for the two most influential variables found in Section 5.4. Data from the cited literature (International Energy Agency, 2021) (Jason Ye, 2021).

	2030	
	Green H_2 (€/kg)	CO_2 (€/kg)
Current state	6.00 – 11.00	0.06 – 0.07
SDS	3.00 – 7.50	0.075 – 0.125
Net zero	1.00 – 3.00	0.11 – 0.15

All LC will be levelled using the base-line operating cost found in Section 5.3. Thereby, a negative result means that the new operating cost of the process is cheaper than the base case, and a positive result means that is more expensive.

Consequently, when the result is positive there is a risk of loss, namely, the base case (air/methane mixture) is economically optimal. Figure 29 shows the risk of loss for every fuel ratio and every forecast scenario. It proves that with the current state legislations and technologic development, the usage of green hydrogen is economically non-viable. Whether the SDS is fully reached, the risk of loss is still quite strong when green hydrogen is employed. Finally, whether the NZE by 2050 scenario is achieved, a volume fraction of 20% and 40% of hydrogen could be considered.

Nevertheless, note that future projections for 2030 state that 100% methane has no risk of loss whatsoever from an economic perspective.

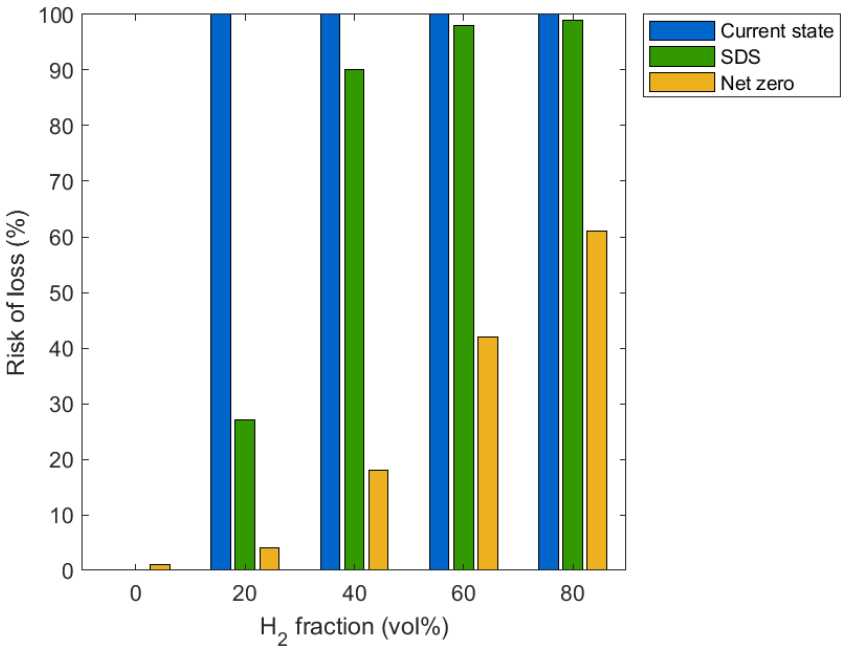

Figure 29. Risk of loss for three different projected scenarios for 2030.

5.6. Life cycle assessment

Consider an industrial water-tube boiler of 44 MW-t power. The fuel requirements for the ratios of study are presented in Table 8.

Table 8. Fuel requirements for the ratios of study.

Hydrogen fraction (vol%)	CH_4 (kWh_{LHV}/kg_{steam})	H_2 (kg/kg_{steam})
0	2.039	0
20	1.803	0.00400
40	1.563	0.00925
60	1.263	0.0168
80	0.827	0.0294

The emission factor for natural gas combustion is 0.164 kg CO_2-e/kWh_{LHV} (Shindell et al., 2013), for natural gas exploration, extraction and distribution in the Spanish market is 0.0508 kg CO_2-e/kWh_{LHV} according to the EcoInvent v3.5 database, and for green hydrogen production via wind energy is 0.970 kg CO_2-e/kg H_2 (Cetinkaya et al., 2012).

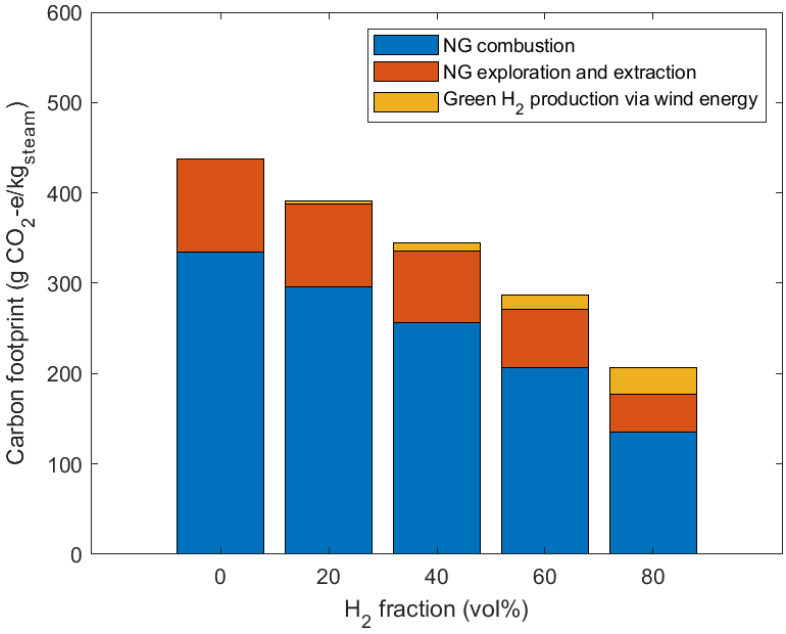

Figure 30. Carbon footprint for an industrial water-tube boiler of 44 MW-t power with different fuel ratios.

According to the results, to produce 1 kg of steam at 200ºC from solely natural gas, roughly 437.8 g CO_2-e are emitted to the atmosphere; whereas, to produce 1 kg of steam from a mixture of 20-80 methane-hydrogen, 206.1 g CO_2-e are produced.

If an 80 vol% hydrogen mixture is used to generate steam, 53% of the carbon emissions can be reduced.

6. Conclusions

This work leads to a better understanding of the potential economic performance and technical feasibility of using HEM as fuel for industrial boilers, under the observed market conditions and expert projections for 2030.

At the studied fuel compositions and considered price levels, there are little incentives to use HEM as fuel. Furthermore, with the current state assumed price levels there is very high probability of risk of loss if hydrogen is employed as fuel. This can be explained by a high production cost of green hydrogen and a low tax on carbon emissions. The same goes for the SDS, there is still high production costs of green hydrogen and little pricing on carbon emissions. Nonetheless, with the NZE by 2050 assumed price levels there is low probability of risk of loss if hydrogen is employed as fuel. This can be explained by a low production cost of green hydrogen (≤3 €/kg H_2) and a high tax on carbon emissions (~0.13 €/kg CO_2).

Green hydrogen is currently seen as an inferior substitute for natural gas (methane) because of its price. Green hydrogen could represent a promising fuel in scenarios where natural gas price is higher than green hydrogen. However, this research has shown that a sustained decline in natural gas prices, as presented in SDS and NZE by 2050 scenario, diminishes significantly the incentives for using green hydrogen as fuel in 2030. These projections suggest a continued decrease in natural gas prices due to carbon taxes and increased shares of renewable energies (International Energy Agency (IEA), 2021). However, recently extreme peaks on natural gas prices in Europe posit great uncertainties and undesirable dependencies (Liang & Thomas, 2022).

Even though the future natural gas and green hydrogen prices are subject of great debate, it is clear that the current energy market presents a high threat on the climate neutrality.

The sensitivity analysis has shown that the economic feasibility of HEM as a fuel for industrial boilers is highly vulnerable to carbon taxes and green hydrogen prices, in that order. This indicates that policy incentives are needed to effectively increase HEM usage.

The results presented above do not include potential economic returns originating from the environmental benefits of using renewable energies. In case these environmental benefits would be monetarized, which is a complex policy issue, the costs would be reduced. Since the usage of green hydrogen is beneficial from an aggregated environmental-economic perspective, several measures could be taken to increase the incentives for private investors. Moreover, higher natural gas prices could be achieved by stronger tax policies on carbon emissions.

One of the limitations of this study is its reliance on Spain gas market conditions. However, the model could be replicated to other territories by replacing the input variables. Moreover, the study does not consider the capital cost of the industrial boiler and other operational costs apart from fuel requirements.

These findings are essential for industry and policymakers by providing important information related to the combustion efficiency, the cost of HEM and the environmental impact to enable climate neutrality.

7. References

Armaroli, D., Bartoloni, F., Brunetto, P., del Vecchio, L., della Chiesa, L., Moraschi, M., Scaramuzzi, M., Varoli, I., Zampini, M., & Napoli, C. (2022). *Global hydrogen trade to meet the 1.5°C climate goal: Part III – Green hydrogen cost and potential*. www.irena.org/publications

ASME PTC 4-2008. (2009). *Fired Steam Generators Performance Test Codes*. http://cstools.asme.org

Bălănescu, D. T., & Homutescu, V. M. (2021). Effects of hydrogen-enriched methane combustion on latent heat recovery potential and environmental impact of condensing boilers. *Applied Thermal Engineering*, *197*. https://doi.org/10.1016/j.applthermaleng.2021.117411

Baukal, C. E. (1998). *Oxygen-enhanced combustion*. CRC Press.

Bion, N., Epron, F., & Duprez, D. (2010). Bioethanol reforming for H_2 production. A comparison with hydrocarbon reforming. In *Catalysis* (pp. 1–55). Royal Society of Chemistry. https://doi.org/10.1039/9781847559630-00001

Cassol, F., Brittes, R., França, F. H. R., & Ezekoye, O. A. (2014). Application of the weighted-sum-of-gray-gases model for media composed of arbitrary concentrations of H2O, CO2 and soot. *International Journal of Heat and Mass Transfer*, *79*, 796–806. https://doi.org/10.1016/j.ijheatmasstransfer.2014.08.032

Cengel, Y. A. (2002). *Heat transfer. A practical approach* (Second).

Cetinkaya, E., Dincer, I., & Naterer, G. F. (2012). Life cycle assessment of various hydrogen production methods. *International Journal of Hydrogen Energy*, *37*(3), 2071–2080. https://doi.org/10.1016/j.ijhydene.2011.10.064

Chang, C. S., Ni, S. H., Yang, H. S., & Chou, C. T. (2021). Simulation study of separating oxygen from air by pressure swing adsorption process with semicylindrical adsorber. *Journal of the Taiwan Institute of Chemical Engineers*, *120*, 67–76. https://doi.org/10.1016/J.JTICE.2021.03.027

Chi, J., & Yu, H. (2018). Water electrolysis based on renewable energy for hydrogen production. *Chinese Journal of Catalysis*, *39*(3), 390–394. https://doi.org/10.1016/S1872-2067(17)62949-8

de Groot, M. T., Kraakman, J., & Garcia Barros, R. L. (2022). Optimal operating parameters for advanced alkaline water electrolysis. *International Journal of Hydrogen Energy*. https://doi.org/10.1016/j.ijhydene.2022.08.075

de Ris, J. (1984). *A Scientific Approach to Flame Radiation and Material Flammability*. Emmons Invited Lecture.

Dukelow, S. G. (1991). *The control of boilers*. Instrument Society of America.

Ebrahimi, H., Zamaniyan, A., Soltan Mohammadzadeh, J. S., & Khalili, A. A. (2013). Zonal modeling of radiative heat transfer in industrial furnaces using simplified model for exchange area calculation. *Applied Mathematical Modelling*, *37*(16–17), 8004–8015. https://doi.org/10.1016/j.apm.2013.02.053

Edwards, D. K. (1976). *Molecular Gas Band Radiation*.

Ersöz, A. (2008). Investigation of hydrocarbon reforming processes for micro-cogeneration systems. *International Journal of Hydrogen Energy*, *33*(23), 7084–7094. https://doi.org/10.1016/J.IJHYDENE.2008.07.062

European Commission. (2020). *A hydrogen strategy for a climate-neutral Europe*. https://www.eu2018.at/calendar-events/political-events/BMNT-

Eyring, V., Gillett, N. P., Achuta Rao, K. M., Barimalala South Africa, R., Barreiro, M., Bock, L., Malinina, E., Ruiz, L., Sallée, J.-B., Santer, B. D., Trewin, B., Weigel, K., Zhang, X., Zhao, A., Halenka, T., Marengo Orsini Brazil, J. A., Mitchell, D., Gillett, N., Achuta Rao, K., … Zhou, B. (2021). *Human Influence on the Climate System*. 423–552. https://doi.org/10.1017/9781009157896.005

Ge, B., Ji, Y., Zhang, Z., Zang, S., Tian, Y., Yu, H., Chen, M., Jiao, G., & Zhang, D. (2019). Experiment study on the combustion performance of hydrogen-enriched natural gas in a DLE burner. *International Journal of Hydrogen Energy*, *44*(26), 14023–14031. https://doi.org/10.1016/j.ijhydene.2019.03.257

George, J. F., Müller, V. P., Winkler, J., & Ragwitz, M. (2022). Is blue hydrogen a bridging technology? - The limits of a CO2 price and the role of state-induced price components for green hydrogen production in Germany. *Energy Policy*, *167*. https://doi.org/10.1016/j.enpol.2022.113072

Götz, M., Lefebvre, J., Mörs, F., McDaniel Koch, A., Graf, F., Bajohr, S., Reimert, R., & Kolb, T. (2016). Renewable Power-to-Gas: A technological and economic review. In *Renewable Energy* (Vol. 85, pp. 1371–1390). Elsevier Ltd. https://doi.org/10.1016/j.renene.2015.07.066

Government of Catalonia. (2022, September 27). Tarragona will have the largest green hydrogen plant in Spain with an investment of 230 million euros. *Http://Catalonia.Com/Newsletter_news/News/2022/Tarragona-Will-Have-the-Largest-Green-Hydrogen-Plant-in-Spain-with-an-Investment-of-230-Million-Euros.Jsp*.

Government of Spain. (2020, October 19). Messer will build a new production plant in Vilaseca. *Https://Www.Investinspain.Org/En/News/2020/Messer-New-Production-Vilaseca*.

Green, Don W, Southard, & Marylee Z. (2019). *Perry's Chemical Engineers' Handbook*.

Green, Don W, Southard, & Marylee Z. (2020). *Perry's Chemical Engineers' Handbook*.

Harnett, J. P. (James P.), & Irvine, T. F. (Thomas F. (1985). *Advances in heat transfer*. Academic Press.

Hawkes, E. R., & Chen, J. H. (2004). Direct numerical simulation of hydrogen-enriched lean premixed methane-air flames. *Combustion and Flame*, *138*(3), 242–258. https://doi.org/10.1016/j.combustflame.2004.04.010

Heselton, K. (2005). *Boiler Operator's Handbook*.

Hottel H.C. (1969). Weighted sum of gray gases model. In *INFORMATION RETRIEVAL* (Vol. 15, Issue 5).

Huisingh, D., Zhang, Z., Moore, J. C., Qiao, Q., & Li, Q. (2015). Recent advances in carbon emissions reduction: Policies, technologies, monitoring, assessment and modeling. *Journal of Cleaner Production*, *103*, 1–12. https://doi.org/10.1016/j.jclepro.2015.04.098

Intergovernmental Panel on Climate Change (IPCC). (2021). *Technical Summary*. https://doi.org/10.1017/9781009157896.002

Intergovernmental Panel on Climate Change (IPCC) Special Report. (2008). *Carbon dioxide capture and storage*.

International Energy Agency, I. (2021). *Global Hydrogen Review 2021*. www.iea.org/t&c/

International Energy Agency (IEA). (2021). *World Energy Model Documentation*.

International Renewable Energy Agency. (2020). *Green Hydrogen Cost Reduction Scaling Up Electrolysers To Meet The 1.5ºC Climate Goal*. www.irena.org/publications

Jaklič, A., Vode, F., & Kolenko, T. (2007). Online simulation model of the slab-reheating process in a pusher-type furnace. *Applied Thermal Engineering*, *27*(5–6), 1105–1114. https://doi.org/10.1016/j.applthermaleng.2006.07.033

Jason Ye. (2021). *Center for Climate and Energy Solutions*.

Kuppens, T., van Dael, M., Vanreppelen, K., Thewys, T., Yperman, J., Carleer, R., Schreurs, S., & van Passel, S. (2015). Techno-economic assessment of fast pyrolysis for the valorization of short rotation coppice cultivated for phytoextraction. *Journal of Cleaner Production*, *88*, 336–344. https://doi.org/10.1016/j.jclepro.2014.07.023

Larrain, M., van Passel, S., Thomassen, G., van Gorp, B., Nhu, T. T., Huysveld, S., van Geem, K. M., de Meester, S., & Billen, P. (2021). Techno-economic assessment of mechanical recycling of challenging post-consumer plastic packaging waste. *Resources, Conservation and Recycling*, *170*. https://doi.org/10.1016/j.resconrec.2021.105607

Lee, B., Heo, J., Kim, S., Sung, C., Moon, C., Moon, S., & Lim, H. (2018). Economic feasibility studies of high pressure PEM water electrolysis for distributed H2 refueling stations. *Energy Conversion and Management*, *162*, 139–144. https://doi.org/10.1016/J.ENCONMAN.2018.02.041

Liang, A., & Thomas, D. (2022, December 5). Ukraine war: Oil prices rise as cap on Russian crude kicks in. *Https://Www.Bbc.Com/News/Business-63855030*.

Lienhard, J. H. (2019). *A Heat Transfer Textbook* (Fifth).

lo Basso, G., Nastasi, B., Astiaso Garcia, D., & Cumo, F. (2017). How to handle the Hydrogen enriched Natural Gas blends in combustion efficiency measurement procedure of conventional and condensing boilers. *Energy*, *123*, 615–636. https://doi.org/10.1016/j.energy.2017.02.042

Ludwig, C. B., Malkmus, W., Reardon, J. E., Thomson, J. A. L., & Goulard, R. (1973). *Handbook of infrared radiation from combustion gases*.

Man, Y., Yang, S., Xiang, D., Li, X., & Qian, Y. (2014). Environmental impact and techno-economic analysis of the coal gasification process with/without CO2

capture. *Journal of Cleaner Production*, *71*, 59–66. https://doi.org/10.1016/j.jclepro.2013.12.086

Mayr, B., Prieler, R., Demuth, M., & Hochenauer, C. (2018). Modelling of high temperature furnaces under air-fuel and oxygen enriched conditions. *Applied Thermal Engineering*, *136*, 492–503. https://doi.org/10.1016/j.applthermaleng.2018.03.013

Modest, M. F., San, N. Y., & London, F. (2013). *Radiative Heat Transfer* (Third). http://elsevier.com/locate/permissions

Muradov, N. Z., & Veziroğlu, T. N. (2005). From hydrocarbon to hydrogen-carbon to hydrogen economy. *International Journal of Hydrogen Energy*, *30*(3), 225–237. https://doi.org/10.1016/j.ijhydene.2004.03.033

Myhre, G., Shindell, D., & Bréon, F. M. (2016). *Global Warming Potential Values*. www.ipcc.ch

Newborough, M., & Cooley, G. (2020). *Developments in the global hydrogen market*.

Nikolaidis, P., & Poullikkas, A. (2017). A comparative overview of hydrogen production processes. In *Renewable and Sustainable Energy Reviews* (Vol. 67, pp. 597–611). Elsevier Ltd. https://doi.org/10.1016/j.rser.2016.09.044

Novak Zuber June, B. (1959). *Hydrodynamic aspects of boiling heating transfer*.

Nukiyama, S. (1934). *The maximum and minimum values of the heat Q transmitted from metal to boiling water under atmospheric pressure*.

Oni, A., Anaya, Y., Giwa, T., di Lullo, G., & Kumar, A. (2022). *Comparative assessment of blue hydrogen from steam methane reforming, autothermal reforming, and natural gas decomposition technologies for natural gas-producing regions*. https://doi.org/10.1016/j.enconman.2022.115245

Optimizer, N. (1981). *GRG2-An All FORTRAN General Purpose*.

Raič, J., Gaber, C., Wachter, P., Demuth, M., Gerhardter, H., Knoll, M., Prieler, R., & Hochenauer, C. (2021). Validation of a coupled 3D CFD simulation model for an oxy-fuel cross-fired glass melting furnace with electric boosting. *Applied Thermal Engineering*, *195*. https://doi.org/10.1016/j.applthermaleng.2021.117166

Raič, J., Wachter, P., Hödl, P., Demuth, M., Gaber, C., Gerhardter, H., Prieler, R., & Hochenauer, C. (2022). CFD simulation aided glass quality and energy efficiency analysis of an oxy-fuel glass melting furnace with electric boosting. *Energy Conversion and Management: X*, *15*, 100252. https://doi.org/10.1016/j.ecmx.2022.100252

Rossmeisl, J., Logadottir, A., & Nørskov, J. K. (2005). Electrolysis of water on (oxidized) metal surfaces. *Chemical Physics*, *319*(1–3), 178–184. https://doi.org/10.1016/j.chemphys.2005.05.038

Shindell, D., Bréon, F., Collins, W., Fuglestvedt, J., Huang, J., Koch, D., Lamarque, J., Lee, D., Mendoza, B., Nakajima, T., Robock, A., Stephens, G., Takemura, T., Zhang, H., Qin, D., Plattner, G., Tignor, M., Allen, S., Boschung, J., … Midgley, P. (2013). *Anthropogenic and Natural Radiative*

Forc-ing. In: Climate Change 2013: The Physical Science Basis. Contribution of Working Group I.

Shiva Kumar, S., & Himabindu, V. (2019a). Hydrogen production by PEM water electrolysis – A review. In *Materials Science for Energy Technologies* (Vol. 2, Issue 3, pp. 442–454). KeAi Communications Co. https://doi.org/10.1016/j.mset.2019.03.002

Shiva Kumar, S., & Himabindu, V. (2019b). Hydrogen production by PEM water electrolysis – A review. In *Materials Science for Energy Technologies* (Vol. 2, Issue 3, pp. 442–454). KeAi Communications Co. https://doi.org/10.1016/j.mset.2019.03.002

Smith, J. M., van Ness, H. C., Abbott, M., & Mark T. (2018). *Introduction to chemical engineering thermodynamics*.

Smith T. F., Shen Z. F., & Friedman J. N. (1982). *Evaluation of Coefficients for the Weighted Sum of Gray Gases Model*. http://heattransfer.asmedigitalcollection.asme.org/

Sørensen, B. (2012). *Hydrogen and Fuel Cells Emerging technologies and applications*. http://energy.ruc.dk

Tang, C., Zhang, Y., & Huang, Z. (2014). Progress in combustion investigations of hydrogen enriched hydrocarbons. In *Renewable and Sustainable Energy Reviews* (Vol. 30, pp. 195–216). Elsevier Ltd. https://doi.org/10.1016/j.rser.2013.10.005

Thomassen, G., van Dael, M., van Passel, S., & You, F. (2019). How to assess the potential of emerging green technologies? Towards a prospective environmental and techno-economic assessment framework. In *Green Chemistry* (Vol. 21, Issue 18, pp. 4868–4886). Royal Society of Chemistry. https://doi.org/10.1039/c9gc02223f

Tong, L. S. (1968). Boundary layer analysis of the flow boiling crisis. *International Journal of Heat and Mass Transfer*, *49*(5–6), 1058–1072. https://doi.org/10.1016/j.ijheatmasstransfer.2005.09.004

Velazquez Abad, A., & Dodds, P. E. (2020). Green hydrogen characterisation initiatives: Definitions, standards, guarantees of origin, and challenges. *Energy Policy*, *138*. https://doi.org/10.1016/j.enpol.2020.111300

Wachtmeister, H., Henke, P., & Höök, M. (2018). Oil projections in retrospect: Revisions, accuracy and current uncertainty. *Applied Energy*, *220*, 138–153. https://doi.org/10.1016/j.apenergy.2018.03.013

Wang, T., Zhang, H., Zhang, Y., Wang, H., Lyu, J., & Yue, G. (2022). Efficiency and emissions of gas-fired industrial boiler fueled with hydrogen-enriched nature gas: A case study of 108 t/h steam boiler. *International Journal of Hydrogen Energy*, *47*(65), 28188–28203. https://doi.org/10.1016/J.IJHYDENE.2022.06.121

Wierzba, I., & Ale, B. B. (2000). *Rich flammability limits of fuel mixtures involving hydrogen at elevated temperatures*.

Yuen, W. W. (2008). Definition and evaluation of mean beam lengths for Applications in multidimensional radiative heat transfer: A mathematically

self-consistent approach. *Journal of Heat Transfer*, *130*(11), 1–5. https://doi.org/10.1115/1.2969752

Yukesh Kannah, R., Kavitha, S., Preethi, Parthiba Karthikeyan, O., Kumar, G., Dai-Viet, N. V., & Rajesh Banu, J. (2021). Techno-economic assessment of various hydrogen production methods – A review. In *Bioresource Technology* (Vol. 319). Elsevier Ltd. https://doi.org/10.1016/j.biortech.2020.124175

Zhang, W., Hibiki, T., Mishima, K., & Mi, Y. (2006). Correlation of critical heat flux for flow boiling of water in mini-channels. *International Journal of Heat and Mass Transfer*, *49*(5–6), 1058–1072. https://doi.org/10.1016/j.ijheatmasstransfer.2005.09.004

Zhang, Y., Jiao, F., Huang, Q., Cao, W., Shi, L., Zhao, M., Yu, C., Nie, B., & Cao, X. (2019). Experimental and numerical studies on the closed and vented explosion behaviors of premixed methane-hydrogen/air mixtures. *Applied Thermal Engineering*, *159*. https://doi.org/10.1016/j.applthermaleng.2019.113907

Zhao, Y., McDonell, V., & Samuelsen, S. (2019a). Influence of hydrogen addition to pipeline natural gas on the combustion performance of a cooktop burner. *International Journal of Hydrogen Energy*, *44*(23), 12239–12253. https://doi.org/10.1016/j.ijhydene.2019.03.100

Zhao, Y., McDonell, V., & Samuelsen, S. (2019b). Experimental assessment of the combustion performance of an oven burner operated on pipeline natural gas mixed with hydrogen. *International Journal of Hydrogen Energy*, *44*(47), 26049–26062. https://doi.org/10.1016/j.ijhydene.2019.08.011

Appendix

A. Specific heat capacity

```
clc
clear all
close all

CpData=readtable("CpAspen.csv","TextType","string");
summary(CpData)
CpData.Properties.VariableNames=["Temperature","Pressure","CpCH4",...
    "CpO2","CpN2","CpCO2","CpH2O","CpH2"];
plot(CpData.Temperature,CpData.CpCH4,'o'),xlabel(CpData.Properties.Var
iableNames(1)+" (°C)"),ylabel("Heat capacity (kJ/kmol·K)")
hold on
plot(CpData.Temperature,CpData{:,4:end},'o')
hold off

pCH4=polyfit(CpData.Temperature,CpData.CpCH4,2);
pO2=polyfit(CpData.Temperature,CpData.CpO2,2);
pN2=polyfit(CpData.Temperature,CpData.CpN2,2);
pCO2=polyfit(CpData.Temperature,CpData.CpCO2,2);
pH2O=polyfit(CpData.Temperature,CpData.CpH2O,2);
pH2=polyfit(CpData.Temperature,CpData.CpH2,2);
polycoef=table(["C3";"C2";"C1"],pCH4',pO2',pN2',pCO2',pH2O',pH2');
polycoef.Properties.VariableNames=["Coefficients","CH4","O2","N2","CO2
","H2O","H2"];

T=1:1:2500;
CppolyCH4=polyval(pCH4,T);
CppolyO2=polyval(pO2,T);
CppolyN2=polyval(pN2,T);
CppolyCO2=polyval(pCO2,T);
CppolyH2O=polyval(pH2O,T);
CppolyH2=polyval(pH2,T);
hold on
plot(T,CppolyCH4), plot(T,CppolyO2), plot(T,CppolyN2)
plot(T,CppolyCO2), plot(T,CppolyH2O), plot(T,CppolyH2)
hold off
legend([CpData.Properties.VariableNames(3:end),'Interpolation'],"Locat
ion","northwest")
```

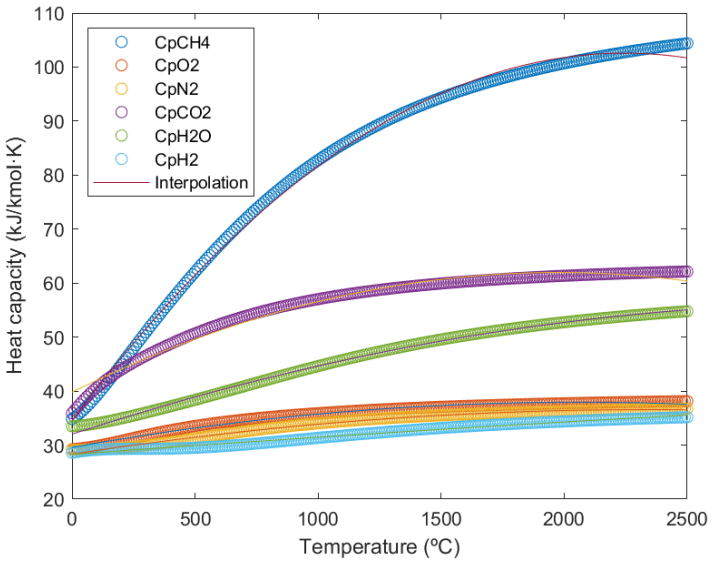

Figure 31. Heat capacity data and interpolation.

Table 9. Heat capacity data from Aspen© at different temperatures.

TEMP	PRES	VAPOR CPIG CH4	VAPOR CPIG O2	VAPOR CPIG N2	VAPOR CPIG CO2	VAPOR CPIG H2O	VAPOR CPIG H2
C	bar	kJ/kmol-K	kJ/kmol-K	kJ/kmol-K	kJ/kmol-K	kJ/kmol-K	kJ/kmol-K
0	1.01325	34.83842	29.24607	29.11605	35.9084	33.48796	28.60358
10	1.01325	35.15166	29.28242	29.1194	36.45216	33.52035	28.67514
20	1.01325	35.49566	29.32402	29.12355	36.98318	33.55757	28.74302
30	1.01325	35.86908	29.37095	29.12864	37.49954	33.59972	28.80689
40	1.01325	36.27031	29.42318	29.1348	37.99991	33.64683	28.86652
50	1.01325	36.69754	29.48065	29.14218	38.48348	33.69888	28.9218
60	1.01325	37.1488	29.54323	29.15091	38.94989	33.75578	28.97266
70	1.01325	37.62206	29.61072	29.16112	39.39915	33.81739	29.01912
80	1.01325	38.11526	29.68289	29.17295	39.83151	33.88354	29.06126
90	1.01325	38.62635	29.75947	29.18651	40.24747	33.95404	29.09919
100	1.01325	39.15336	29.84016	29.20191	40.6477	34.02864	29.13309
110	1.01325	39.69436	29.92463	29.21926	41.03295	34.10711	29.16313
120	1.01325	40.24756	30.01255	29.23863	41.40407	34.1892	29.18954
130	1.01325	40.81125	30.10358	29.26009	41.76193	34.27463	29.21254
140	1.01325	41.38388	30.19736	29.28371	42.10742	34.36316	29.23238
150	1.01325	41.96398	30.29356	29.30953	42.44143	34.45452	29.24932
160	1.01325	42.55026	30.39184	29.33757	42.76482	34.54847	29.26361
170	1.01325	43.14151	30.49187	29.36785	43.0784	34.64478	29.2755
180	1.01325	43.73665	30.59333	29.40036	43.38295	34.74321	29.28526
190	1.01325	44.33474	30.69593	29.43511	43.67919	34.84357	29.29314
200	1.01325	44.93491	30.79938	29.47205	43.9678	34.94567	29.29937
210	1.01325	45.53641	30.90341	29.51116	44.24939	35.04931	29.3042
220	1.01325	46.13857	31.00777	29.5524	44.52452	35.15436	29.30785
230	1.01325	46.74081	31.11223	29.5957	44.7937	35.26066	29.31054
240	1.01325	47.34262	31.21659	29.641	45.05738	35.36809	29.31247
250	1.01325	47.94356	31.32064	29.68824	45.31597	35.47654	29.31385
260	1.01325	48.54323	31.42421	29.73734	45.56984	35.58591	29.31485
270	1.01325	49.14131	31.52714	29.78822	45.8193	35.69611	29.31564
280	1.01325	49.7375	31.62929	29.84079	46.06463	35.80708	29.31639
290	1.01325	50.33155	31.73053	29.89497	46.30608	35.91876	29.31724
300	1.01325	50.92325	31.83075	29.95067	46.54386	36.0311	29.31833
310	1.01325	51.5124	31.92985	30.0078	46.77816	36.14405	29.31979
320	1.01325	52.09885	32.02776	30.06625	47.00913	36.25759	29.32172
330	1.01325	52.68245	32.12439	30.12595	47.23691	36.37169	29.32424
340	1.01325	53.26308	32.21968	30.1868	47.46163	36.48633	29.32743
350	1.01325	53.84063	32.31359	30.2487	47.68336	36.60149	29.33138
360	1.01325	54.41499	32.40608	30.31156	47.9022	36.71716	29.33615
370	1.01325	54.98609	32.49711	30.3753	48.11822	36.83334	29.34183
380	1.01325	55.55384	32.58666	30.43983	48.33148	36.95003	29.34845

390	1.01325	56.11817	32.67471	30.50506	48.54202	37.06721	29.35607
400	1.01325	56.67902	32.76125	30.57091	48.74989	37.18489	29.36473
410	1.01325	57.23632	32.84628	30.6373	48.95511	37.30306	29.37446
420	1.01325	57.79001	32.9298	30.70415	49.15772	37.42174	29.38528
430	1.01325	58.34005	33.01182	30.77138	49.35774	37.5409	29.39723
440	1.01325	58.88638	33.09233	30.83894	49.55519	37.66056	29.4103
450	1.01325	59.42894	33.17136	30.90673	49.75009	37.78071	29.42451
460	1.01325	59.9677	33.24892	30.97472	49.94244	37.90135	29.43987
470	1.01325	60.50261	33.32503	31.04281	50.13227	38.02248	29.45638
480	1.01325	61.03361	33.3997	31.11097	50.31959	38.14408	29.47402
490	1.01325	61.56068	33.47297	31.17913	50.5044	38.26615	29.49279
500	1.01325	62.08376	33.54485	31.24724	50.68672	38.38869	29.51268
510	1.01325	62.60282	33.61538	31.31525	50.86656	38.51168	29.53367
520	1.01325	63.11782	33.68456	31.38311	51.04393	38.63511	29.55575
530	1.01325	63.62872	33.75245	31.45077	51.21884	38.75898	29.5789
540	1.01325	64.13548	33.81905	31.5182	51.39131	38.88325	29.60309
550	1.01325	64.63808	33.8844	31.58535	51.56133	39.00792	29.6283
560	1.01325	65.13648	33.94853	31.65219	51.72894	39.13297	29.6545
570	1.01325	65.63065	34.01146	31.71869	51.89414	39.25839	29.68167
580	1.01325	66.12057	34.07322	31.78481	52.05695	39.38414	29.70977
590	1.01325	66.6062	34.13384	31.85052	52.21739	39.51021	29.73878
600	1.01325	67.08752	34.19336	31.91579	52.37546	39.63658	29.76867
610	1.01325	67.56451	34.25178	31.98061	52.5312	39.76322	29.79941
620	1.01325	68.03715	34.30916	32.04494	52.68461	39.89011	29.83096
630	1.01325	68.50542	34.36549	32.10877	52.83573	40.01723	29.86329
640	1.01325	68.9693	34.42083	32.17208	52.98456	40.14454	29.89637
650	1.01325	69.42878	34.47518	32.23484	53.13113	40.27202	29.93017
660	1.01325	69.88385	34.52859	32.29705	53.27546	40.39965	29.96466
670	1.01325	70.3345	34.58106	32.35869	53.41758	40.52739	29.99979
680	1.01325	70.78072	34.63262	32.41974	53.55751	40.65522	30.03555
690	1.01325	71.22251	34.6833	32.4802	53.69526	40.78311	30.0719
700	1.01325	71.65986	34.73312	32.54005	53.83088	40.91103	30.1088
710	1.01325	72.09277	34.78211	32.59929	53.96438	41.03896	30.14623
720	1.01325	72.52124	34.83027	32.6579	54.09578	41.16686	30.18415
730	1.01325	72.94528	34.87764	32.71589	54.22512	41.2947	30.22254
740	1.01325	73.36489	34.92423	32.77324	54.35242	41.42247	30.26136
750	1.01325	73.78007	34.97007	32.82996	54.4777	41.55013	30.30059
760	1.01325	74.19084	35.01516	32.88603	54.601	41.67765	30.3402
770	1.01325	74.59721	35.05954	32.94146	54.72234	41.805	30.38016
780	1.01325	74.99919	35.10321	32.99625	54.84174	41.93217	30.42044
790	1.01325	75.39679	35.1462	33.05038	54.95924	42.05911	30.46101
800	1.01325	75.79003	35.18851	33.10387	55.07487	42.18582	30.50186
810	1.01325	76.17893	35.23018	33.15671	55.18864	42.31225	30.54295
820	1.01325	76.5635	35.2712	33.20891	55.30059	42.43839	30.58426
830	1.01325	76.94377	35.31161	33.26046	55.41074	42.56421	30.62577

840	1.01325	77.31976	35.3514	33.31136	55.51913	42.68969	30.66745
850	1.01325	77.69149	35.3906	33.36163	55.62577	42.8148	30.70929
860	1.01325	78.05898	35.42922	33.41126	55.7307	42.93952	30.75126
870	1.01325	78.42227	35.46727	33.46025	55.83395	43.06384	30.79333
880	1.01325	78.78138	35.50476	33.50861	55.93553	43.18772	30.8355
890	1.01325	79.13633	35.54172	33.55635	56.03549	43.31115	30.87774
900	1.01325	79.48716	35.57813	33.60346	56.13383	43.4341	30.92003
910	1.01325	79.83389	35.61403	33.64996	56.2306	43.55657	30.96236
920	1.01325	80.17657	35.64942	33.69584	56.32582	43.67852	31.0047
930	1.01325	80.51521	35.68431	33.74112	56.4195	43.79995	31.04704
940	1.01325	80.84985	35.71872	33.78579	56.51169	43.92083	31.08937
950	1.01325	81.18053	35.75264	33.82987	56.6024	44.04115	31.13167
960	1.01325	81.50727	35.7861	33.87335	56.69165	44.16089	31.17393
970	1.01325	81.83012	35.8191	33.91626	56.77948	44.28004	31.21612
980	1.01325	82.1491	35.85164	33.95858	56.86591	44.39858	31.25825
990	1.01325	82.46426	35.88375	34.00033	56.95096	44.5165	31.30029
1000	1.01325	82.77563	35.91542	34.04151	57.03466	44.63379	31.34224
1010	1.01325	83.08325	35.94667	34.08213	57.11702	44.75043	31.38407
1020	1.01325	83.38714	35.9775	34.1222	57.19808	44.86642	31.42579
1030	1.01325	83.68736	36.00792	34.16173	57.27785	44.98173	31.46738
1040	1.01325	83.98394	36.03794	34.20071	57.35636	45.09637	31.50883
1050	1.01325	84.27691	36.06757	34.23916	57.43364	45.21032	31.55013
1060	1.01325	84.56631	36.09681	34.27708	57.50969	45.32356	31.59127
1070	1.01325	84.85218	36.12567	34.31448	57.58455	45.43611	31.63224
1080	1.01325	85.13457	36.15416	34.35137	57.65823	45.54793	31.67304
1090	1.01325	85.4135	36.18228	34.38775	57.73077	45.65904	31.71366
1100	1.01325	85.68901	36.21004	34.42363	57.80216	45.76941	31.75409
1110	1.01325	85.96115	36.23745	34.45902	57.87245	45.87905	31.79433
1120	1.01325	86.22996	36.26451	34.49392	57.94164	45.98795	31.83436
1130	1.01325	86.49546	36.29122	34.52834	58.00975	46.0961	31.87418
1140	1.01325	86.75771	36.31761	34.56229	58.07682	46.20349	31.91379
1150	1.01325	87.01673	36.34366	34.59577	58.14284	46.31013	31.95318
1160	1.01325	87.27257	36.36938	34.62879	58.20785	46.41601	31.99234
1170	1.01325	87.52526	36.39479	34.66135	58.27187	46.52113	32.03128
1180	1.01325	87.77484	36.41988	34.69347	58.3349	46.62548	32.06998
1190	1.01325	88.02136	36.44466	34.72515	58.39697	46.72906	32.10844
1200	1.01325	88.26484	36.46914	34.75639	58.45809	46.83186	32.14667
1210	1.01325	88.50532	36.49332	34.7872	58.51828	46.93389	32.18465
1220	1.01325	88.74285	36.5172	34.8176	58.57756	47.03515	32.22238
1230	1.01325	88.97746	36.54079	34.84757	58.63595	47.13563	32.25986
1240	1.01325	89.20918	36.5641	34.87714	58.69345	47.23533	32.29709
1250	1.01325	89.43805	36.58712	34.9063	58.75009	47.33425	32.33406
1260	1.01325	89.66411	36.60987	34.93507	58.80589	47.4324	32.37078
1270	1.01325	89.8874	36.63235	34.96344	58.86084	47.52976	32.40723
1280	1.01325	90.10795	36.65455	34.99143	58.91499	47.62635	32.44343

1290	1.01325	90.32579	36.6765	35.01904	58.96832	47.72216	32.47936
1300	1.01325	90.54096	36.69818	35.04627	59.02087	47.8172	32.51503
1310	1.01325	90.7535	36.7196	35.07314	59.07264	47.91146	32.55043
1320	1.01325	90.96344	36.74077	35.09964	59.12365	48.00495	32.58556
1330	1.01325	91.17081	36.76169	35.12579	59.17391	48.09766	32.62043
1340	1.01325	91.37565	36.78237	35.15158	59.22344	48.18961	32.65503
1350	1.01325	91.57799	36.8028	35.17703	59.27225	48.28079	32.68936
1360	1.01325	91.77787	36.823	35.20213	59.32034	48.3712	32.72343
1370	1.01325	91.97531	36.84296	35.2269	59.36774	48.46085	32.75722
1380	1.01325	92.17035	36.86269	35.25134	59.41446	48.54975	32.79074
1390	1.01325	92.36302	36.88219	35.27545	59.4605	48.63788	32.824
1400	1.01325	92.55336	36.90147	35.29925	59.50588	48.72526	32.85699
1410	1.01325	92.74139	36.92052	35.32272	59.55062	48.8119	32.8897
1420	1.01325	92.92715	36.93936	35.34589	59.59471	48.89778	32.92215
1430	1.01325	93.11067	36.95797	35.36875	59.63818	48.98292	32.95433
1440	1.01325	93.29197	36.97638	35.39131	59.68104	49.06733	32.98625
1450	1.01325	93.47109	36.99458	35.41357	59.72329	49.15099	33.01789
1460	1.01325	93.64805	37.01257	35.43554	59.76494	49.23393	33.04928
1470	1.01325	93.8229	37.03036	35.45722	59.80602	49.31614	33.08039
1480	1.01325	93.99564	37.04794	35.47862	59.84651	49.39762	33.11124
1490	1.01325	94.16632	37.06533	35.49974	59.88645	49.47839	33.14183
1500	1.01325	94.33497	37.08252	35.52059	59.92583	49.55844	33.17216
1510	1.01325	94.5016	37.09952	35.54116	59.96466	49.63778	33.20223
1520	1.01325	94.66625	37.11633	35.56147	60.00297	49.71642	33.23203
1530	1.01325	94.82894	37.13295	35.58152	60.04074	49.79435	33.26158
1540	1.01325	94.9897	37.14939	35.60131	60.078	49.87159	33.29087
1550	1.01325	95.14856	37.16564	35.62084	60.11475	49.94814	33.3199
1560	1.01325	95.30555	37.18171	35.64013	60.151	50.024	33.34868
1570	1.01325	95.46068	37.19761	35.65916	60.18675	50.09918	33.37721
1580	1.01325	95.61399	37.21333	35.67796	60.22203	50.17369	33.40548
1590	1.01325	95.76549	37.22888	35.69652	60.25683	50.24752	33.4335
1600	1.01325	95.91523	37.24425	35.71484	60.29116	50.32068	33.46128
1610	1.01325	96.0632	37.25946	35.73293	60.32504	50.39319	33.48881
1620	1.01325	96.20946	37.27451	35.7508	60.35846	50.46503	33.51609
1630	1.01325	96.35401	37.28938	35.76843	60.39144	50.53623	33.54313
1640	1.01325	96.49687	37.3041	35.78585	60.42398	50.60678	33.56992
1650	1.01325	96.63808	37.31866	35.80305	60.4561	50.67669	33.59648
1660	1.01325	96.77766	37.33306	35.82004	60.48779	50.74596	33.6228
1670	1.01325	96.91562	37.3473	35.83681	60.51906	50.8146	33.64888
1680	1.01325	97.052	37.3614	35.85338	60.54993	50.88262	33.67472
1690	1.01325	97.1868	37.37534	35.86974	60.5804	50.95002	33.70033
1700	1.01325	97.32006	37.38913	35.8859	60.61047	51.0168	33.72571
1710	1.01325	97.45179	37.40277	35.90187	60.64016	51.08297	33.75086
1720	1.01325	97.58202	37.41627	35.91763	60.66946	51.14854	33.77579
1730	1.01325	97.71077	37.42962	35.93321	60.69838	51.21351	33.80048

1740	1.01325	97.83805	37.44283	35.94859	60.72694	51.27788	33.82495
1750	1.01325	97.96388	37.45591	35.96379	60.75513	51.34167	33.8492
1760	1.01325	98.08829	37.46884	35.9788	60.78297	51.40487	33.87323
1770	1.01325	98.2113	37.48164	35.99363	60.81045	51.4675	33.89704
1780	1.01325	98.33292	37.4943	36.00829	60.83758	51.52955	33.92063
1790	1.01325	98.45317	37.50683	36.02277	60.86438	51.59104	33.944
1800	1.01325	98.57207	37.51923	36.03707	60.89084	51.65196	33.96717
1810	1.01325	98.68965	37.5315	36.0512	60.91696	51.71232	33.99012
1820	1.01325	98.80591	37.54365	36.06517	60.94277	51.77214	34.01286
1830	1.01325	98.92088	37.55566	36.07897	60.96825	51.8314	34.0354
1840	1.01325	99.03457	37.56755	36.09261	60.99342	51.89013	34.05772
1850	1.01325	99.147	37.57932	36.10608	61.01828	51.94831	34.07985
1860	1.01325	99.25818	37.59097	36.1194	61.04283	52.00597	34.10177
1870	1.01325	99.36815	37.6025	36.13256	61.06708	52.0631	34.12349
1880	1.01325	99.4769	37.61391	36.14557	61.09104	52.11971	34.14502
1890	1.01325	99.58446	37.6252	36.15842	61.11471	52.1758	34.16634
1900	1.01325	99.69084	37.63637	36.17113	61.13809	52.23137	34.18747
1910	1.01325	99.79606	37.64744	36.18369	61.16118	52.28645	34.20841
1920	1.01325	99.90013	37.65839	36.1961	61.184	52.34102	34.22916
1930	1.01325	100.0031	37.66922	36.20837	61.20655	52.39509	34.24972
1940	1.01325	100.1049	37.67995	36.2205	61.22883	52.44867	34.27009
1950	1.01325	100.2056	37.69057	36.23249	61.25084	52.50176	34.29027
1960	1.01325	100.3053	37.70109	36.24434	61.27259	52.55437	34.31027
1970	1.01325	100.4038	37.71149	36.25606	61.29408	52.60651	34.33009
1980	1.01325	100.5013	37.7218	36.26765	61.31532	52.65817	34.34973
1990	1.01325	100.5978	37.732	36.2791	61.33631	52.70936	34.36919
2000	1.01325	100.6933	37.7421	36.29043	61.35706	52.76009	34.38847
2010	1.01325	100.7877	37.75209	36.30163	61.37756	52.81035	34.40758
2020	1.01325	100.8811	37.76199	36.3127	61.39783	52.86017	34.42651
2030	1.01325	100.9735	37.77179	36.32365	61.41786	52.90953	34.44527
2040	1.01325	101.065	37.78149	36.33447	61.43765	52.95845	34.46387
2050	1.01325	101.1555	37.7911	36.34518	61.45722	53.00693	34.48229
2060	1.01325	101.245	37.80061	36.35577	61.47657	53.05497	34.50055
2070	1.01325	101.3336	37.81003	36.36624	61.49569	53.10258	34.51864
2080	1.01325	101.4213	37.81936	36.37659	61.5146	53.14976	34.53656
2090	1.01325	101.508	37.82859	36.38683	61.53329	53.19651	34.55433
2100	1.01325	101.5939	37.83774	36.39696	61.55177	53.24285	34.57194
2110	1.01325	101.6788	37.84679	36.40698	61.57004	53.28877	34.58938
2120	1.01325	101.7629	37.85576	36.41689	61.58811	53.33428	34.60667
2130	1.01325	101.8461	37.86464	36.42669	61.60597	53.37939	34.62381
2140	1.01325	101.9285	37.87344	36.43639	61.62363	53.42409	34.64079
2150	1.01325	102.01	37.88215	36.44598	61.6411	53.46839	34.65762
2160	1.01325	102.0907	37.89077	36.45547	61.65837	53.5123	34.67429
2170	1.01325	102.1705	37.89932	36.46485	61.67545	53.55582	34.69082
2180	1.01325	102.2496	37.90778	36.47414	61.69235	53.59895	34.7072

2190	1.01325	102.3278	37.91616	36.48333	61.70905	53.6417	34.72344
2200	1.01325	102.4053	37.92446	36.49241	61.72558	53.68407	34.73953
2210	1.01325	102.4819	37.93268	36.50141	61.74192	53.72607	34.75547
2220	1.01325	102.5578	37.94083	36.51031	61.75809	53.76769	34.77128
2230	1.01325	102.6329	37.94889	36.51911	61.77408	53.80895	34.78694
2240	1.01325	102.7073	37.95689	36.52782	61.78989	53.84984	34.80247
2250	1.01325	102.7809	37.9648	36.53644	61.80554	53.89038	34.81786
2260	1.01325	102.8538	37.97264	36.54497	61.82102	53.93056	34.83311
2270	1.01325	102.926	37.98041	36.55341	61.83633	53.97038	34.84822
2280	1.01325	102.9974	37.9881	36.56176	61.85148	54.00986	34.86321
2290	1.01325	103.0682	37.99573	36.57003	61.86646	54.04899	34.87806
2300	1.01325	103.1382	38.00328	36.57821	61.88129	54.08779	34.89278
2310	1.01325	103.2075	38.01076	36.58631	61.89596	54.12624	34.90737
2320	1.01325	103.2762	38.01817	36.59432	61.91048	54.16436	34.92184
2330	1.01325	103.3442	38.02552	36.60226	61.92484	54.20215	34.93617
2340	1.01325	103.4115	38.03279	36.61011	61.93905	54.23961	34.95039
2350	1.01325	103.4782	38.04	36.61788	61.95312	54.27674	34.96448
2360	1.01325	103.5442	38.04714	36.62557	61.96703	54.31355	34.97844
2370	1.01325	103.6096	38.05422	36.63319	61.98081	54.35005	34.99229
2380	1.01325	103.6744	38.06123	36.64072	61.99444	54.38623	35.00601
2390	1.01325	103.7385	38.06818	36.64819	62.00792	54.4221	35.01961
2400	1.01325	103.802	38.07507	36.65557	62.02128	54.45766	35.0331
2410	1.01325	103.8649	38.08189	36.66289	62.03449	54.49292	35.04647
2420	1.01325	103.9272	38.08865	36.67013	62.04757	54.52788	35.05973
2430	1.01325	103.9889	38.09535	36.6773	62.06051	54.56253	35.07287
2440	1.01325	104.05	38.10199	36.68439	62.07333	54.59689	35.0859
2450	1.01325	104.1106	38.10857	36.69142	62.08601	54.63096	35.09881
2460	1.01325	104.1705	38.11509	36.69838	62.09856	54.66474	35.11162
2470	1.01325	104.2299	38.12155	36.70527	62.11099	54.69823	35.12431
2480	1.01325	104.2888	38.12796	36.71209	62.1233	54.73144	35.1369
2490	1.01325	104.347	38.13431	36.71884	62.13548	54.76437	35.14938
2500	1.01325	104.4048	38.1406	36.72553	62.14754	54.79702	35.16175

B. Aspen EDR© combustion results

	COMBUSTION DESIGN CONDITIONS						
1	Type of fuel		Fuel Mix	Fuel 1	Fuel 2	Fuel 3	Fuel 4
2	Fuel flowrate	kg/s	0.88	0.88			
3	Excess air, %		10				
4	Calculated heat release (LHV)	kW	44009.3				
5	Calculated fuel efficiency (LHV), %		52.58032				
6	Flue gas temp leaving: Radiant sect.	°C	947				
7	: Convection	°C	947				
8	: Air preheater	°C					
9	Flue gas quantity (wet)	kg/s	17.5249				
10	Flue gas mass vel. (bank1-bank5)	kg/s/m²					
11	Flue gas mass vel. (bank6-bank9)	kg/s/m²					
12	Draft at arch	bar	0.01008				
13	Draft at burners	bar	0.00836				
14	Ambient air temp. (efficiency calc.)	°C	10				
15	Ambient air temp. (stack design)	°C	10				
16	**FUEL CHARACTERISTICS:**						
17	Type of fuel		Fuel Mix	Fuel 1	Fuel 2	Fuel 3	Fuel 4
18	Fuel lower calorific value (LHV)	kJ/kg	50010.6	50010.6			
19	Temperature @ burner	°C		25			
20	Composition (mass fraction)						
21	Carbon	-	0.7487	0.7487			
22	Hydrogen	-	0.2513	0.2513			
23	Oxygen	-	0	0			
24	Nitrogen	-	0	0			
25	Sulphur	-	0	0			
26	Ash	-	0	0			
27	**BURNER DATA:**						
28	Type		forced draught standard (HTFS)		Number	1	
29	Heat release per burner	kW	44009.3		Location	bottom	

Figure 32. Combustion design conditions with 0 vol% hydrogen content.

	COMBUSTION DESIGN CONDITIONS						
1	Type of fuel		Fuel Mix	Fuel 1	Fuel 2	Fuel 3	Fuel 4
2	Fuel flowrate	kg/s	0.8444	0.8444			
3	Excess air, %		10				
4	Calculated heat release (LHV)	kW	44030.2				
5	Calculated fuel efficiency (LHV), %		52.83332				
6	Flue gas temp leaving: Radiant sect.	°C	949				
7	: Convection	°C	949				
8	: Air preheater	°C					
9	Flue gas quantity (wet)	kg/s	17.2982				
10	Flue gas mass vel. (bank1-bank5)	kg/s/m²					
11	Flue gas mass vel. (bank6-bank9)	kg/s/m²					
12	Draft at arch	bar	0.00989				
13	Draft at burners	bar	0.00817				
14	Ambient air temp. (efficiency calc.)	°C	10				
15	Ambient air temp. (stack design)	°C	10				
16	**FUEL CHARACTERISTICS:**						
17	Type of fuel		Fuel Mix	Fuel 1	Fuel 2	Fuel 3	Fuel 4
18	Fuel lower calorific value (LHV)	kJ/kg	52141	52141			
19	Temperature @ burner	°C		25			
20	Composition (mass fraction)						
21	Carbon	-	0.7259	0.7259			
22	Hydrogen	-	0.2741	0.2741			
23	Oxygen	-	0	0			
24	Nitrogen	-	0	0			
25	Sulphur	-	0	0			
26	Ash	-	0	0			
27	**BURNER DATA:**						
28	Type		forced draught standard (HTFS)		Number	1	
29	Heat release per burner	kW	44030.2		Location	bottom	

Figure 33. Combustion design conditions with 20 vol% hydrogen content.

	COMBUSTION DESIGN CONDITIONS						
1	Type of fuel		Fuel Mix	Fuel 1	Fuel 2	Fuel 3	Fuel 4
2	Fuel flowrate	kg/s	0.7944	0.7944			
3	Excess air, %		10				
4	Calculated heat release (LHV)	kW	44025.8				
5	Calculated fuel efficiency (LHV), %		53.19081				
6	Flue gas temp leaving: Radiant sect.	°C	951				
7	: Convection	°C	951				
8	: Air preheater	°C					
9	Flue gas quantity (wet)	kg/s	16.9704				
10	Flue gas mass vel. (bank1-bank5)	kg/s/m²					
11	Flue gas mass vel. (bank6-bank9)	kg/s/m²					
12	Draft at arch	bar	0.00961				
13	Draft at burners	bar	0.00788				
14	Ambient air temp. (efficiency calc.)	°C	10				
15	Ambient air temp. (stack design)	°C	10				
16	**FUEL CHARACTERISTICS:**						
17	Type of fuel		Fuel Mix	Fuel 1	Fuel 2	Fuel 3	Fuel 4
18	Fuel lower calorific value (LHV)	kJ/kg	55417.2	55417.2			
19	Temperature @ burner	°C		25			
20	Composition (mass fraction)						
21	Carbon	-	0.6908	0.6908			
22	Hydrogen	-	0.3092	0.3092			
23	Oxygen	-	0	0			
24	Nitrogen	-	0	0			
25	Sulphur	-	0	0			
26	Ash	-	0	0			
27	**BURNER DATA:**						
28	Type		forced draught standard (HTFS)		Number	1	
29	Heat release per burner	kW	44025.8		Location	bottom	

Figure 34. Combustion design conditions with 40 vol% hydrogen content.

	COMBUSTION DESIGN CONDITIONS						
1	Type of fuel		Fuel Mix	Fuel 1	Fuel 2	Fuel 3	Fuel 4
2	Fuel flowrate	kg/s	0.7208	0.7208			
3	Excess air, %		10				
4	Calculated heat release (LHV)	kW	44045.4				
5	Calculated fuel efficiency (LHV), %		53.70929				
6	Flue gas temp leaving: Radiant sect.	°C	956				
7	: Convection	°C	956				
8	: Air preheater	°C					
9	Flue gas quantity (wet)	kg/s	16.4948				
10	Flue gas mass vel. (bank1-bank5)	kg/s/m²					
11	Flue gas mass vel. (bank6-bank9)	kg/s/m²					
12	Draft at arch	bar	0.00921				
13	Draft at burners	bar	0.00748				
14	Ambient air temp. (efficiency calc.)	°C	10				
15	Ambient air temp. (stack design)	°C	10				
16	**FUEL CHARACTERISTICS:**						
17	Type of fuel		Fuel Mix	Fuel 1	Fuel 2	Fuel 3	Fuel 4
18	Fuel lower calorific value (LHV)	kJ/kg	61103.5	61103.5			
19	Temperature @ burner	°C		25			
20	Composition (mass fraction)						
21	Carbon	-	0.6299	0.6299			
22	Hydrogen	-	0.3701	0.3701			
23	Oxygen	-	0	0			
24	Nitrogen	-	0	0			
25	Sulphur	-	0	0			
26	Ash	-	0	0			
27	**BURNER DATA:**						
28	Type		forced draught standard (HTFS)		Number	1	
29	Heat release per burner	kW	44045.4		Location	bottom	

Figure 35. Combustion design conditions with 60 vol% hydrogen content.

	COMBUSTION DESIGN CONDITIONS						
1	Type of fuel		Fuel Mix	Fuel 1	Fuel 2	Fuel 3	Fuel 4
2	Fuel flowrate	kg/s	0.6	0.6			
3	Excess air, %		10				
4	Calculated heat release (LHV)	kW	44044.3				
5	Calculated fuel efficiency (LHV), %		54.55656				
6	Flue gas temp leaving: Radiant sect.	°C	963				
7	: Convection	°C	963				
8	: Air preheater	°C					
9	Flue gas quantity (wet)	kg/s	15.7051				
10	Flue gas mass vel. (bank1-bank5)	kg/s/m²					
11	Flue gas mass vel. (bank6-bank9)	kg/s/m²					
12	Draft at arch	bar	0.00857				
13	Draft at burners	bar	0.00682				
14	Ambient air temp. (efficiency calc.)	°C	10				
15	Ambient air temp. (stack design)	°C	10				
16	**FUEL CHARACTERISTICS:**						
17	Type of fuel		Fuel Mix	Fuel 1	Fuel 2	Fuel 3	Fuel 4
18	Fuel lower calorific value (LHV)	kJ/kg	73407.2	73407.2			
19	Temperature @ burner	°C		25			
20	Composition (mass fraction)						
21	Carbon	-	0.4982	0.4982			
22	Hydrogen	-	0.5018	0.5018			
23	Oxygen	-	0	0			
24	Nitrogen	-	0	0			
25	Sulphur	-	0	0			
26	Ash	-	0	0			
27	**BURNER DATA:**						
28	Type		forced draught standard (HTFS)		Number	1	
29	Heat release per burner	kW	44044.3		Location	bottom	

Figure 36. Combustion design conditions with 80 vol% hydrogen content.

C. P-H diagram

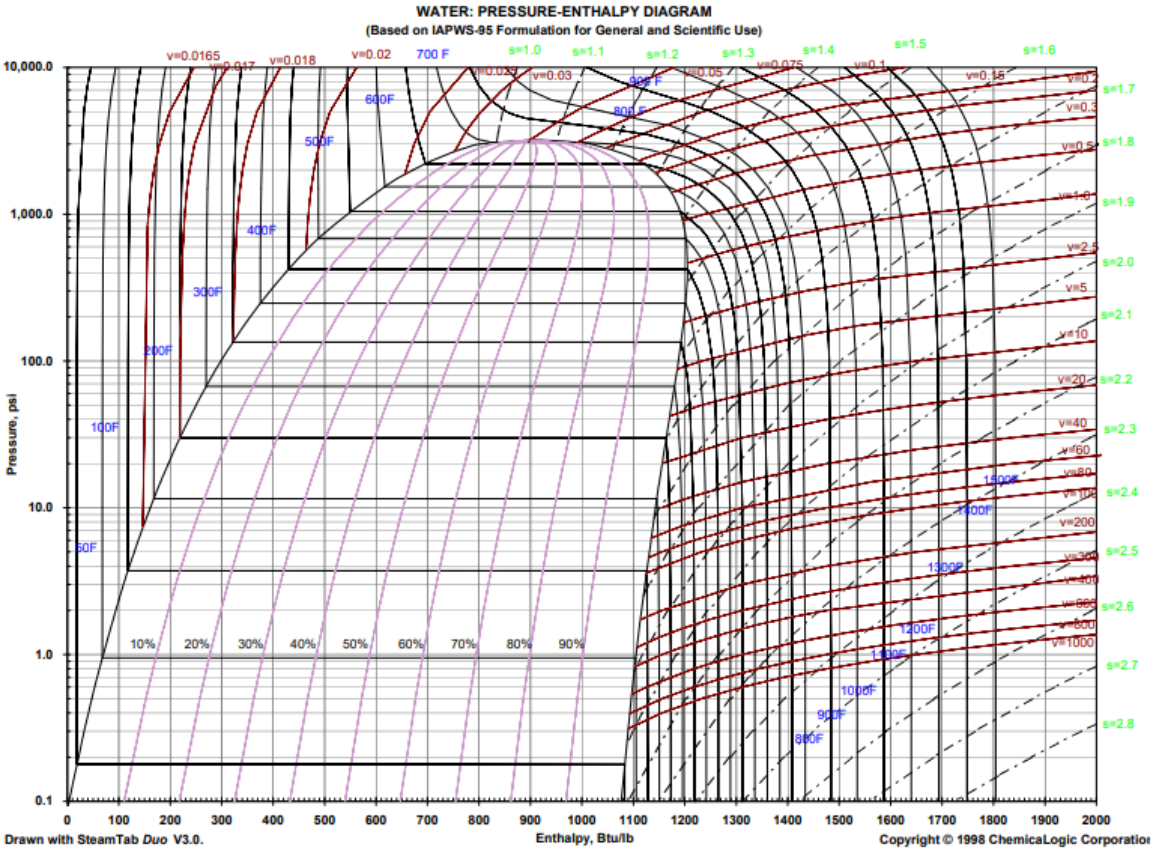

Figure 37. Pressure-enthalpy diagram of water (H_2O).

D. Self-evaluation questionnaire

Evaluate the acquired competences according to the tasks you have carried out.

Degree Competences		Task in which you have observed the competence	Self-evaluation [Rank 1 to 10]	Aspects to be improved
SPECIFIC COMPETENCES				
A1.1	Effectively apply knowledge of basic, scientific and technological materials pertaining to engineering.	Thermodynamic model of a furnace. Thermodynamic model of a boiler.	10	-
A1.2	Design, execute and analyse experiments related to engineering	-	-	-
A1.3	Be able to analyse and synthesize the continuous progress of products, processes, systems and services, whilst applying criteria of safety, economic viability, quality and environmental management. (G6)	Economic feasibility of a hydrogen-enriched industrial boiler. Environmental impact of an industrial boiler.	9	Other variables could be considered, such as labour costs, feedstock costs, etc.
A1.4	Know how to establish and develop mathematical models by using the appropriate software in order to provide the scientific and technological basis for the design of new products, processes, systems and services and for the optimization of existing ones. (G5)	Fitting a polynomial equation into available specific heat capacity data.	9	More advanced equations could have been used. However, for the aim of this work it seemed sufficient.
A2.1	Be able to apply the scientific method	Thermodynamic model of a	9	More specifications and hence a closer approach

	and the principles of engineering and economics to formulate and solve complex problems that arise in processes, equipment, installations and services, in which the material undergoes changes to its composition, state or energy content, these changes being characteristic of industrial chemistry and other related sectors such as pharmacology, biotechnology, materials sciences, energy, food and the environment. (G1)	firebox. Simulation of a fired heater.		to reality could have been considered. However, for the aim of this work it seemed sufficient.
A2.2	Conceive, project, calculate and design processes, equipment, industrial installations and services in the field of chemical engineering and related industrial sectors in terms of quality, safety, economics, the rational and efficient use of natural resources and the conservation of the environment. (G2)	Thermodynamic model of a firebox. Economic assessment of an industrial boiler. Environmental impact study.	10	-
A2.3	Lead and technically and economically manage projects, installations, plants, companies and technological centres in the ambit of chemical engineering and	-	-	-

	related industrial sectors. (G3)			
A3.1	Apply knowledge of mathematics, physics, chemistry, biology and other natural sciences by means of study, experience, practice and critical reasoning in order to establish economically viable solutions for technical problems (I1).	Techno-economic assessment of an industrial boiler.	10	-
A3.2	Design and optimize products, processes, systems and services for the chemical industry on the basis of various areas of chemical engineering, including processes, transport, separation operations, and chemical, nuclear, electrochemical and biochemical reactions engineering (I2).	-	-	-
A3.3	Conceptualize engineering models and apply innovative problems solving methods and appropriate IT applications to the design, simulation, optimization and control of processes and systems (I3).	Thermodynamic model of a firebox using Excel. Simulation of a Fired heater using Aspen EDR©.	10	-
A3.4	Be able to solve unfamiliar and ill-defined problems by taking into account all possible solutions and selecting the most innovative. (I4)	Thermal radiation model for a firebox.	10	-

A3.5	Lead and supervise all types of installation, process, system and service in the different industrial areas related to chemical engineering (I5).	-	-	-
A3.6	Design, construct and implement methods, processes and installations for the integrated management of waste, solids, liquids and gases, whilst also taking into account the impacts and risks of these products (I6).	-	-	-
A4.1	Lead and organize companies and production and service systems by applying knowledge and abilities regarding industrial organization, commercial strategy, planning and logistics, mercantile and labour legislation, and financial and costs accounting (P1).	-	-	-
A4.2	Lead and manage the organization of work and human resources by applying criteria regarding industrial safety, quality management, occupation risk prevention, sustainability and environmental management (P2).	-	-	-
A4.3	Manage research, development and	State-of-the-art of hydrogen	10	-

	technological innovation whilst ensuring the transfer of technology and taking into account property and patent rights (P3).	technologies. State-of-the-art of combustion.		
A4.4	Adapt to structural changes in society caused by economic, energy or natural factors so as to be able to solve any resulting problems and to contribute technological solutions with a high commitment to sustainability (P4).	Techno-economic assessment. Market study of natural gas, electricity and green hydrogen.	10	-
A4.5	Lead and monitor the control of installations, processes, products, certification, auditing, verification, testing and reports (P5).	-	-	-
A5.1	Carry out, present and defend (once all the curriculum credits have been obtained) an original individually produced piece of work before a university panel. The work will consist of a professional integrated Chemical Engineering project that synthesizes (TFM1)	Techno-economic assessment of a hydrogen-enriched boiler of 44 MW-t power.	10	-
TRANSVERSAL COMPETENCES				
B1.1	Communicate and discuss proposals and conclusions in a clear and unambiguous manner in specialized and non-	Participate in monthly meetings.	9	In some cases, visual material that supported the message could have been useful.

	specialized multilingual forums (G9).			
B1.2	Adapt to changes and be able to apply new and advanced technologies and other important developments with initiative and entrepreneurial spirit. (G10)	Application of new thermodynamic models and new technology.	8	CFD programs were not used to simulate processes.
B2.1	Lead and define multidisciplinary teams that are able to make technical changes and address management needs in national and international contexts. (G8)	-	-	-
B3.1	Work in a team with responsibilities shared among multidisciplinary, multilingual and multicultural teams	Being part of the Applications team and working with the sales department.	8	Few multicultural teams were encountered.
B4.1	Be able to learn autonomously in order to maintain and improve the competences pertaining to chemical engineering that enable continuous professional development. (G11)	Specific meetings with Messer Group GmbH regarding thermal radiation in a furnace.	9	Competences were improved, but not as independently as intended.
B5.1	Carry out and lead the appropriate research, design and development of engineering solutions in new or little understood areas, whilst applying criteria of creativity, originality, innovation and	Industrial boiler fuelled with HEM.	9	Other innovative approaches could have been used, such as CFD programs. However, little research can be found on industrial boilers fuelled with HEM.

	technology transfer. (G4)			
B5.2	Bring together knowledge, make judgements and take decisions on the basis of incomplete or limited knowledge whilst taking into account the social and ethical responsibilities of professional practice. (G7)	Environmental impact of an industrial boiler.	8	Ethical responsibilities were not considered.
NUCLEAR COMPETENCES				
C1.1	Have an intermediate mastery of a foreign language, preferably English	Meetings with Messer Group GmbH carried out in English. Some documentation only available in German.	10	-
C1.2	Be advanced users of the information and communication technologies	Master's thesis carried out using different software (Excel Solver and Aspen EDR©)	9	CFD programs were not employed.
C1.3	Be able to manage information and knowledge	Techno-economic assessment of an industrial boiler	10	-
C1.4	Be able to express themselves correctly both orally and in writing in one of the two official languages of the URV	Meeting within Messer Ibérica de Gases.	10	-
C2.1	Be committed to ethics and social responsibility as citizens and professionals	Open forum on safety as a fundamental pillar of the chemical industry.	10	-

C2.2	Be able to define and develop their academic and professional project	Proactive behaviour in the assignment of projects.	10	-

Evaluate the final master project and suggest improvements.

Key steps	**Evaluation [Mark 1 to 10]**	**Improvement proposed**
Selection/assignment of the project (dissemination, communication, assignment requirements...)	10	-
Stay (welcome, length, relationship, follow-up made by the company...)	10	-
Follow-up made by URV tutor	10	-
Other aspects to be considered (which ones...)	-	-